Comprehensive FE numerical insight into Finale Emilia Castle behavior under 2012 Emilia Romagna seismic sequence: Damage causes and seismic vulnerability mitigation hypothesis

Simone Tiberti [a], Maurizio Acito [b], Gabriele Milani [b,*]

[a] *Technical University of Milan, Piazza Leonardo da Vinci 32, 20133, Italy*
[b] *Dept. of Architecture, Built Environment and Construction Engineering, Technical University of Milan, Piazza Leonardo da Vinci 32, 20133 Milan, Italy*

ABSTRACT

In this paper, a numerical insight on the historical masonry Castle of Finale Emilia, symbol of the conse-quences occurred after the seismic sequence of 20–29th May 2012 in Emilia Romagna, Italy, is presented.

Some different numerical models are critically compared, in order to both have an insight into the causes at the base of the partial collapse of the structure and propose valuable rehabilitation interven-tions with seismic upgrading to prevent future damage under seismic loads. Two different meshes are utilized, the one very refined and constituted by tetrahedron elements, the other much coarser and mainly constituted by hexahedrons, along with different hypotheses presented for the masonry material (linear and elasto-plastic with damage and softening).

The analyses performed include standard modal, nonlinear static (pushover) and nonlinear dynamic analyses, under different hypotheses concerning the material properties of the single walls. Three different configurations are compared, the first is the real one stricken by the earthquake (where only one of the walls had been consolidated), the second is a hypothetical castle without any consolidated wall, the last is the situation that should be encountered after full rehabilitation. At this aim, full three-dimensional (3D) detailed finite element models (FEM) are adopted, starting from the available documentation at disposal (photos and existing drawings).

From numerical results, it is found that the insufficient resistance of the constituent materials is mostly responsible for the damages observed and that the partial rehabilitation implemented by the municipality on one wall helped in limiting the damaging effect of the seismic sequence. In all cases, the numerical analyses provide a valuable picture of active damage mechanisms, giving useful hints for the reconstruc-tion and indicating that a limited upgrading of masonry mechanical properties could limit considerably the global seismic vulnerability of the structure, in light of a reconstruction of the collapsed parts of the Castle.

1. Introduction

The Technical University of Milan, with scientific responsibility by two of the authors (Acito and Milani), has been commissioned by the Italian Ministry of Cultural Heritage and Activities and Tourism (MiBACT) with the task to perform wide and comprehensive numerical analyses aimed at better understanding the causes behind the collapse of many complex masonry monuments in Finale Emilia, Italy, occurred during the May 2012 seismic events and subsequent aftershocks. Finale Emilia is one of the villages within the area struck by the Emilia Romagna 2012 seismic sequence which suffered the most for the consequences of the earthquake.

The most important part of the research project, which is also its final aim, is to propose reconstruction guidelines for all those masonry structures whose restoration has been deemed paramount, detailed with advanced FE numerical models. The aforementioned masonry structures include a selection of masonry towers, castles and churches that should apparently be rebuilt exactly as they were before the seismic event, but with a much lower seismic vulnerability.

Only recently the Italian regulations for constructions [1–3] have classified as seismic zone a relevant part of the Italian

* Corresponding author. Tel.: +39 3495516064.
E-mail address: gabriele.milani@polimi.it (G. Milani).

Published Journal Article available at: http://dx.doi.org/10.1016/j.engstruct.2016.02.048

territory previously unclassified, including also the portion of the Emilia Romagna region struck by the earthquake, where the structures are indeed located.

Moreover, specific guidelines for the built heritage [4] are available for all those specialists involved in the safety assessment of monumental masonry structures. They can certainly be considered among the most advanced guidelines in the world, focused on monumental masonry buildings. Specifically, they deal with detailed yet simplified assessments of masonry towers and churches, mainly based either on equilibrium concepts within the no-tension material hypotheses or on the kinematic theorem of limit analysis applied on pre-assigned failure mechanisms with no-tension materials. Such architectural typologies are undoubt-edly the most diffused in the built Italian architectural heritage stock, which a variety of different studies has focused on [5–11].

Nevertheless, there are other interesting cases that do not fit such features. As a matter of fact, very generic indications for masonry castles are available [12–19] but a detailed methodology of approach is unfortunately still not regulated, also because each building presents a unique architectural plant, a common feature in such kind of structures. The present work can therefore be considered as one of the first advanced numerical assessments of a real case relying into a castle severely damaged by the earthquake, and aimed both at a detailed evaluation of the seismic vulnerability of the structure, and at providing design indications for a correct reconstruction of the damaged parts of the building and for a proper mitigation of the seismic vulnerability.

As a matter of fact, the assessment of historical buildings/castles/churches seismic performance is still an open and difficult issue. Historic masonry structures exhibit peculiar characteristics

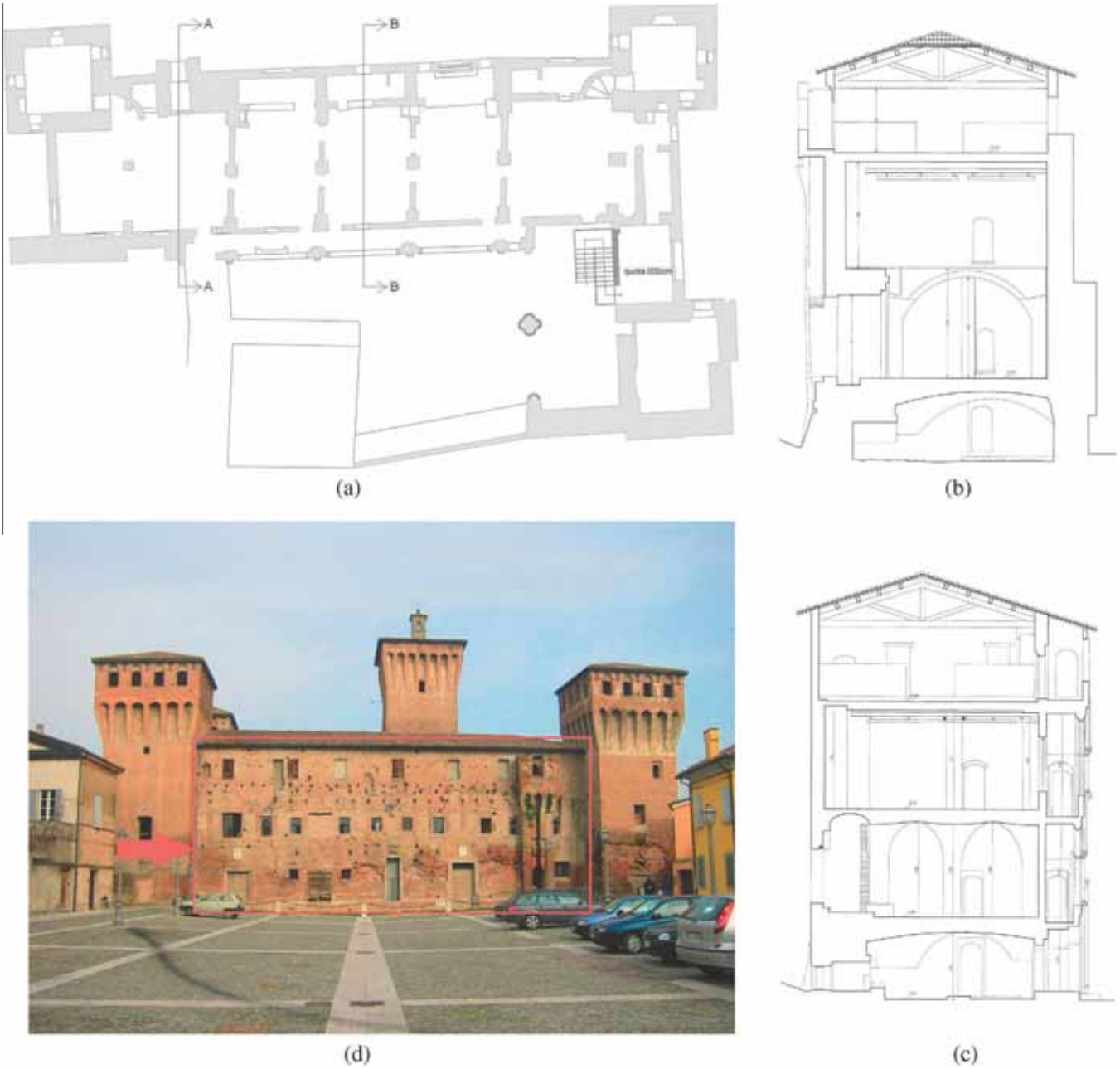

Fig. 1. Clockwise, (a) view plan of the Castle, (b) section AA, (c) section BB and (d) front view of the Castle with the main façade squared in red. (For interpretation of the references to color in this figure legend, the reader is referred to the web version of this article.)

that make their analyses with standard design and generalist assessment methods (similar to the ones currently used for reinforced concrete) definitely unsuited. Few papers recommending specific seismic analyses for the safety assessment of historical or existing buildings/churches without box behavior are available for instance in [20–23], but according to authors' experience, the research is still open for castles, that are peculiar structures needing dedicated numerical approaches.

The monument under investigation belongs to the latter category. It is the so-called "Castello delle Rocche", from here ongoing "the Castle", pictured in Fig. 1 and subject of a few extensive studies [24,25]. The Castle, which is constituted by an L-shaped main building and an independent Main Tower (in Italian named "Mastio", Fig. 2a and b), exhibits important crack patterns and partial collapses mainly on the upper part of the towers (Fig. 2c and d) located on the corners. Conversely, the Main Tower is totally collapsed, yet it is not the object of the present investigation being it a totally independent structure. A comprehensive mapping of cracks and damages is shown in Fig. 3.

The Castle is located at one of the extremes of the ancient walled town of Finale Emilia, located in correspondence of the river Panaro, not far from its confluence into the much larger river Po. During the Medieval age Finale Emilia was a small but strategically important town of the Estense Dukedom (whose capital city was Ferrara), due to its position with respect to the morphology of the Dukedom itself; in fact, the latter exhibited a clepsydra shape, and Finale Emilia was located in the middle of the clepsydra along with the nearby town of San Felice sul Panaro. Then, from Finale it was possible to control the passage of the goods transported through the river and at the same time strategically defend the Dukedom in case of war by the neighboring countries (Bologna and Mirandola).

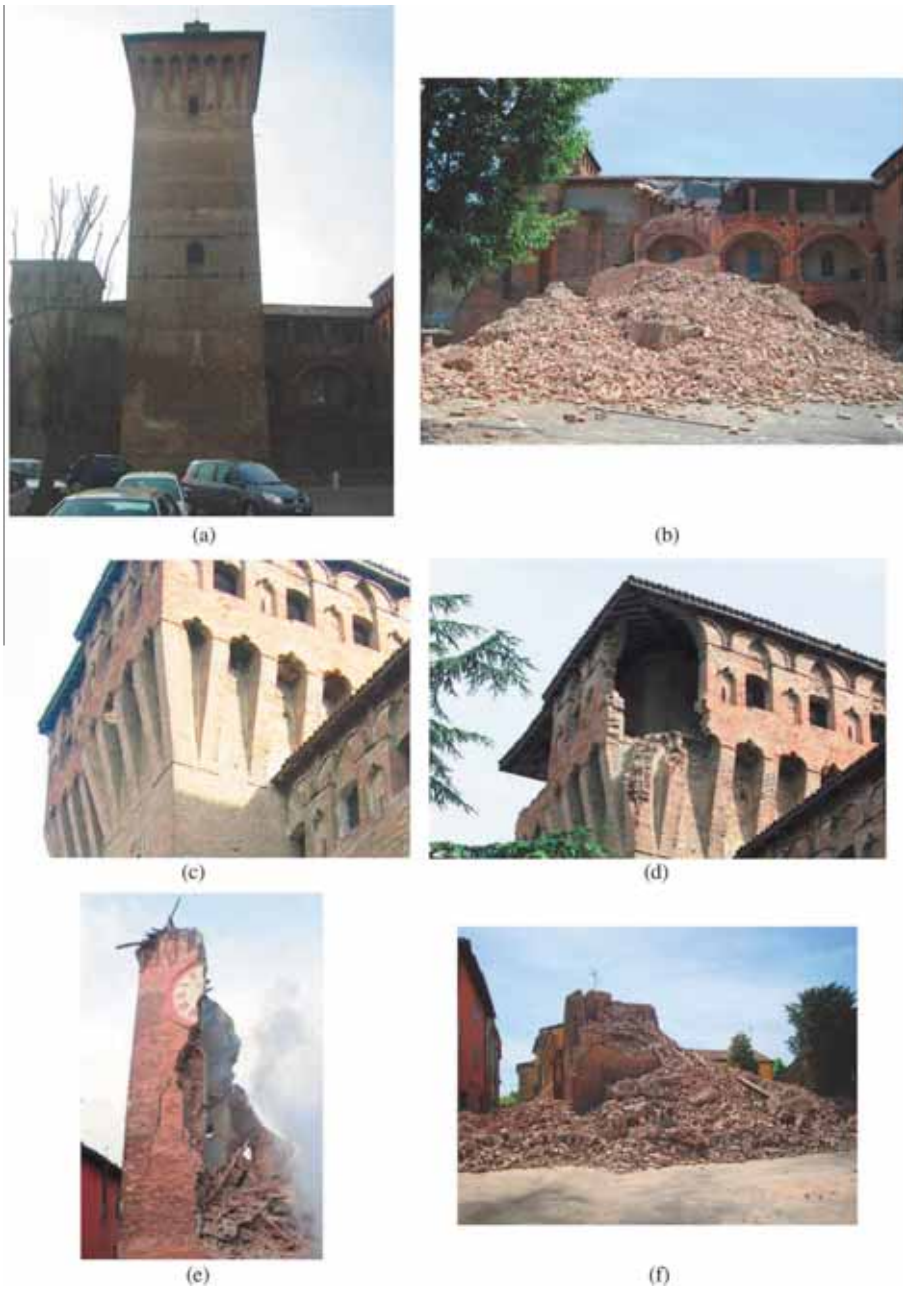

Fig. 2. Before and after the May 20th shock for (a and b) the Main Tower, (c and d) the West Tower of the Castle and (e and f) the Clock Tower.

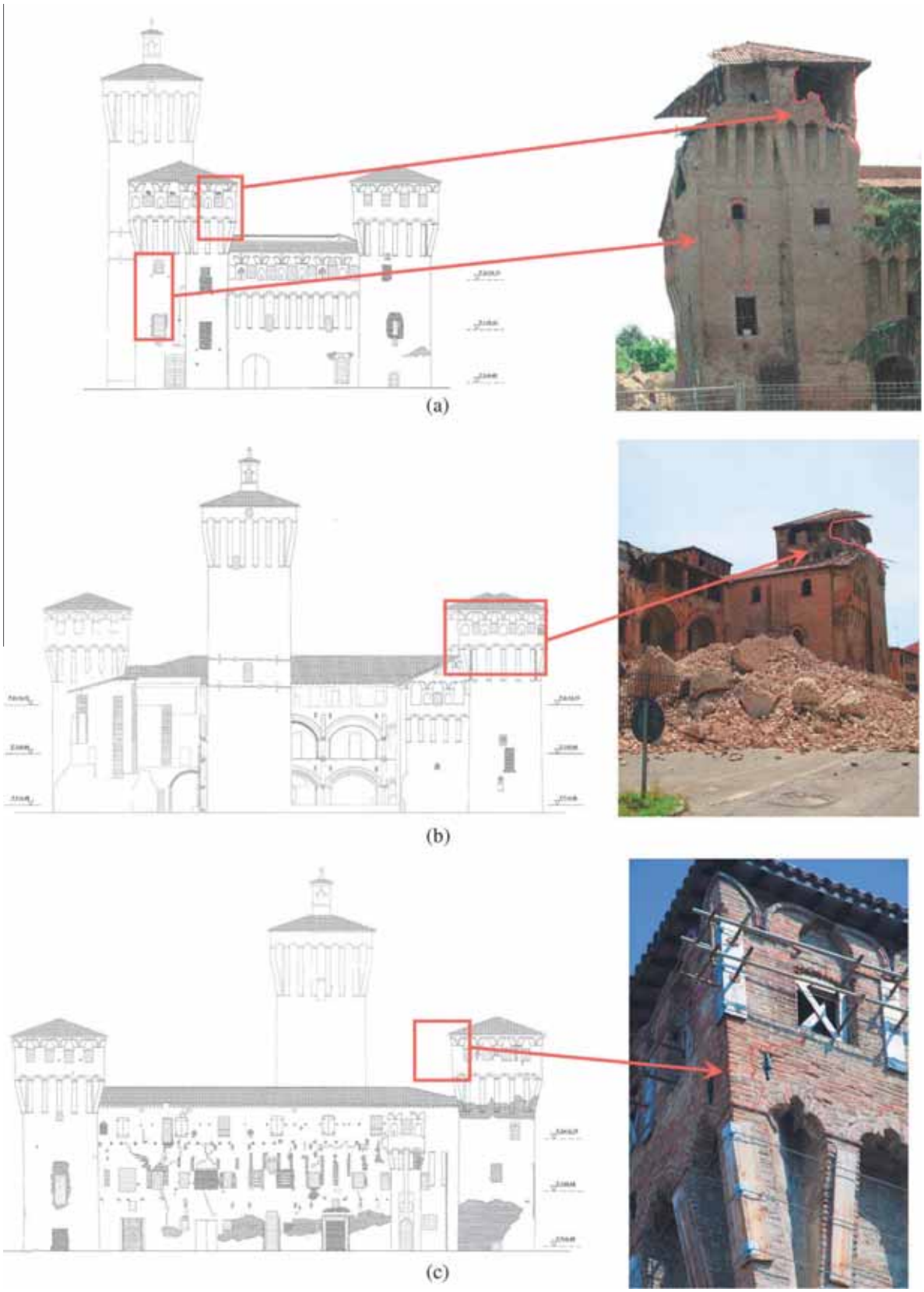

Fig. 3. Corner out-of-plane overturning and cracks in the West Tower (a, seen from Southwest), out-of-plane overturning in the West Tower (b, seen from Northwest) and cracks in the East tower (c).

A tower (later known as the Clock Tower) and a fortified castle were located at the extremes of the walled city, in correspondence of the river. The control of the goods and ships passage occurred therefore with a twofold check conducted in both directions, from the tower and the Castle.

During the last centuries, the town underwent substantial changes, because of the progressive loss of strategic importance of the Dukedom: the walls do not exist anymore, whereas the river has been deviated for public health reasons.

The 2012 earthquake caused the total collapse of both the Clock Tower (Fig. 2e and f, which became the symbol of the earthquake due to the huge amount of pictures of its precarious equilibrium conditions after the main shock available, showing one half of the structure still non-collapsed near the other collapsed into ruins) and the Main Tower of the Castle, as well diffused damages on the upper parts of the three towers of the Castle, with the partial collapse of the upper part of the tower oriented to West.

Fig. 4. Two couples of steel beams are present in each room situated on the longer arm of the Castle; one couple runs along opposite walls and the other is aimed at linking the first two beams.

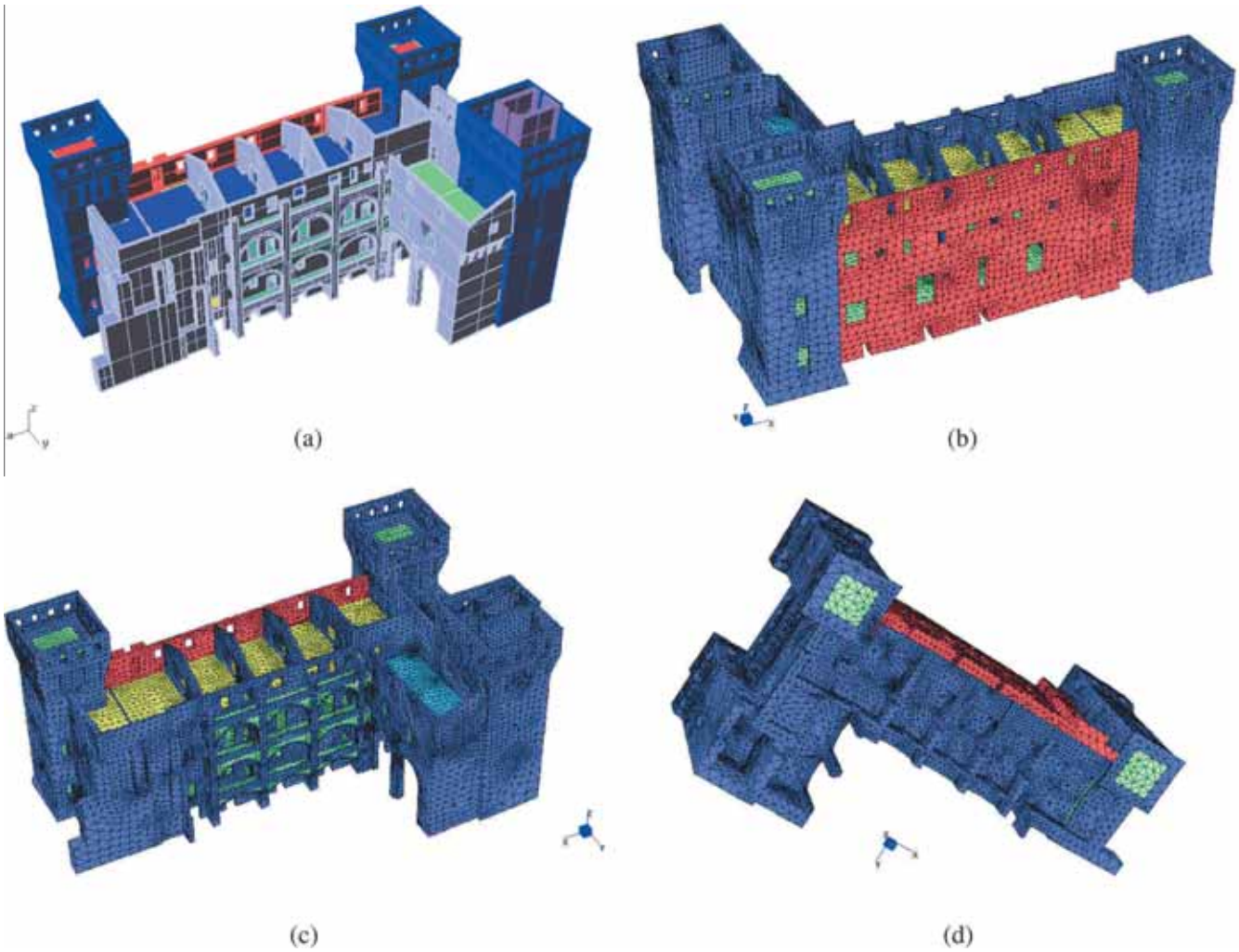

Fig. 5. (a) Virtual geometrical model and (b, c and d) FE model utilized for modal and nonlinear dynamic analyses, tetrahedron elements (Mesh 1).

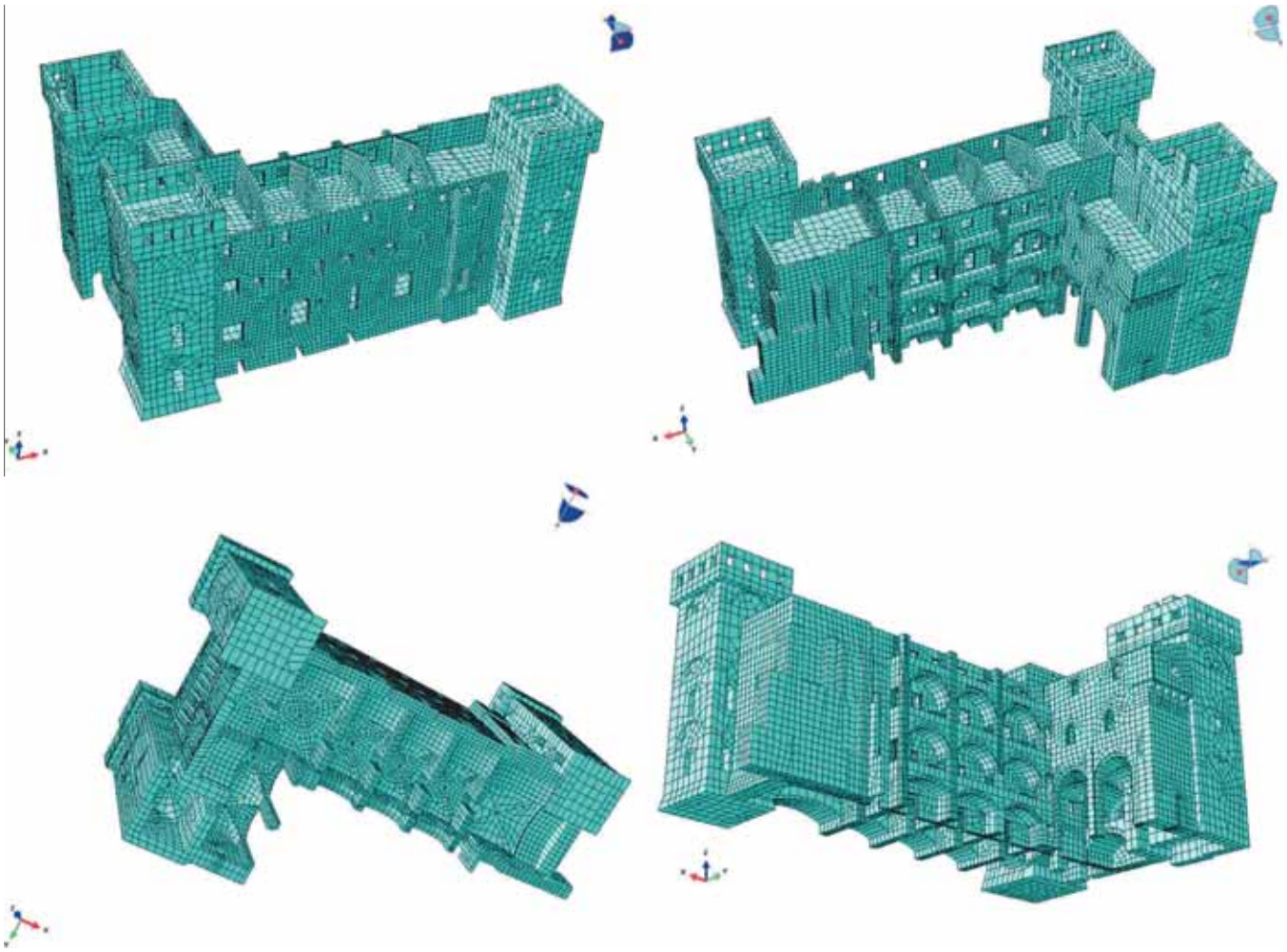

Fig. 6. Hexahedral FE model used for the pushover analyses (Mesh 2).

Table 1
Mechanical elastic properties and densities assigned to the different parts of the Castle.

Material	Density ρ (kg/m^3)	Young modulus E (MPa)
Restored masonry	1800	1500
Non-restored masonry	1800	900
Vaults infill	1600	600
Concrete-and-bricks	2000	25,000
Wood	1000	10,000

Throughout the Sixties the Castle underwent some restoration works, consisting in the substitution of the masonry floors in the second story of the longer arm of the building with new ones made of concrete-and-clay blocks and the strengthening of a few masonry walls with the indenting technique. Other renovations occurred in the Nineties, while the most recent one – and the most important too – took place in 2009, mainly involving the main façade located southeast: damaged portions of the masonry were substituted with the indenting technique and tendons were inserted into the wall thickness.

In the present paper, the final results of advanced numerical analyses conducted on different detailed 3D FE discretized models of the Castle are presented and discussed in detail. They comprise (1) modal analyses with two different meshes and commercial codes (Strand7 [26] and ABAQUS [27]), (2) nonlinear pushover analyses by means of an advanced nonlinear material model and

Table 2
Stress–inelastic strain values utilized in the CDP model for masonry within ABAQUS.

Restored masonry			
Compression		Tension	
$\varepsilon_{plastic}$	σ (MPa)	$\varepsilon_{plastic}$	σ (MPa)
0	2.4	0	0.08
0.005	2.1	0.005	0.0005
0.01	2.1	0.1	0.0005
0.1	1.8		
		Damage in tension	
		$\varepsilon_{plastic}$	d_t
		0	0
		0.005	0.95
Non-restored masonry			
Compression		Tension	
$\varepsilon_{plastic}$	σ (MPa)	$\varepsilon_{plastic}$	σ (MPa)
0	1.22	0	0.04
0.005	0.95	0.003	0.0005
0.01	0.95	0.1	0.0005
0.1	0.8		
		Damage in tension	
		$\varepsilon_{plastic}$	d_t
		0	0
		0.003	0.95

(3) full nonlinear dynamic analyses with input accelerogram registered during the 20th May seismic event. Pushover is conducted by means of the commercial code ABAQUS [27], assuming a Concrete Damaged Plasticity model for masonry with isotropic damage in both tension and compression.

Attention is focused on the interpretation of the collapse modalities induced by the seismic actions. Three hypotheses are critically compared, one representing the real situation encountered during the seismic event (from here ongoing called "real case"), i.e. with only one external wall (shown in Fig. 1d) along the West–East axis restored, a hypothetical situation where no restoration is present (from here ongoing called "non-restored case") and a final hypothesis where it is assumed that the restoration done in 2009 has been extended to the whole structure (hereafter called "fully-restored case").

The numerical results obtained can provide useful design/restoration hints related to the expected seismic behavior of the castle after a hypothetical reconstruction of the collapsed parts obtained by means of lime masonries with improved mechanical properties.

2. Numerical models

Advanced numerical computations are carried out by means of two distinct FE models, one constituted by a quite refined mesh with tetrahedron elements (requiring huge computation effort to be performed in nonlinear computations), the other less detailed and generally constituted by hexahedron elements.

Modeling the floors has always been a very relevant issue when dealing with numerical models. In this case, the second story concrete-and-clay floors were modeled as rigid floors, as they are indeed properly tied to the masonry walls. This results from the restoration works done in the Sixties; actually, tying between floors and walls was strengthened by devising a frame of steel beams for each room, which is depicted in Fig. 4. In the aftermath of the earthquake it was observed that neither detaching nor damages occurred between floors and walls, which are instead common features in old masonry buildings struck by a seismic sequence; no consequence whatsoever occurred in this case even considering the relatively high strength of the shake and its damaging effects observed on a larger scale in neighboring structures, hence the reason for which the floors were modeled as rigid.

The FE tetra and hexahedral discretizations adopted are shown in Figs. 5 and 6, respectively. Both are obtained after a suitable 3D geometric virtual model of the Castle is conceived into Rhinoceros, see Fig. 5a. As a matter of fact, the number of rows present along the thickness for both meshes is variable due to the automatic routines. Only on the last floor, where particularly thin walls are present, a single row of elements is used, to properly connect such walls with previous story ones. However, on average three rows of elements are present, which is a fair compromise between numerical efficiency and the possibility to reproduce properly the out-of-plane behavior even in the nonlinear range.

Some additional details of the numerical models used are provided hereafter:

(1) Mesh 1 with tetrahedrons is obtained by means of Strand7 auto-meshing feature. It is composed by 93,063 nodes and 395,765 elements and it has been used for modal analyses within Strand7. The same 3D model has been then exported into ABAQUS code – passing from Nastran – in order to perform nonlinear dynamic analyses with the damage plasticity model available in such code. Authors experienced, indeed, that the less refined model constituted by hexahedrons, see following point, is unsuitable for the nonlinear dynamic analyses.

(2) Mesh 2 mainly constituted by hexahedrons (along with few wedge elements to secure continuity) is obtained by directly importing into ABAQUS different parts of a simplified geometrical Rhinoceros model, each one characterized by a different material. Each part, after being meshed, was tied with the contiguous ones by using the eponymous feature available in ABAQUS; eventually it was subdivided in smaller cells in order to be able to at least partially exploit the auto-meshing feature of the software. Such operation was however not possible for all the cells, so that almost half of them were meshed manually. While apparently it seems that there are topology errors at the common edges of two contiguous cells, ties available into ABAQUS secure the displacements continuity at the interfaces. The discretization is constituted by 63,435 nodes and 39,207 elements (3467 of which are wedges) and it has been used for modal and pushover analyses. The mesh is much less refined than the previous one and allows faster computations. A comparison between modal performances gives an idea of the accuracy of the results obtained with the second mesh, while limited to the linear elastic range. Mesh 2 has been also created in order to investigate its potential as a less-refined mesh in terms of reduction of the analyses computational cost and its reliability in representing the real structure in the nonlinear range. A series of pushover analyses were also successfully performed on it, the model featuring excellent convergence when compared with Mesh 1. Authors experienced a particularly noticeable stress concentration in correspondence of openings, intersections between perpendicular walls and sharp changes of the dimensions of the elements in Mesh 2, even in the linear elastic range. This is typical of unrefined meshes and such issue makes the latter discretization unsuitable when dealing with nonlinear dynamic analyses. Moreover, authors experienced a much robust behavior when the refinement of Mesh 2 is doubled. Such refinement requires however computational times much higher with respect to those observed for Mesh 1, and is linked with output results rather similar. For this reason, only Mesh 1 is adopted for nonlinear dynamic analyses, but where possible Mesh 2 is preferred in order to speed up computations.

3. Material properties

As far as the masonry properties are concerned, two different materials have been taken into account: one for the masonry of the main façade, characterized by a higher Young modulus and a higher strength both in tension and compression, and one for the masonry of the remaining part of the Castle, see Tables 1 and 2. When dealing with the inelastic damage plasticity laws used into ABAQUS Concrete Damaged Plasticity model (CDP), values assumed are summarized in Table 2, where the wall subjected to restoring interventions during 2009 goes under the name "restored masonry", while the rest is named "non-restored masonry".

Mechanical properties adopted for the non-restored masonry were obtained by using some experimental data conducted on coeval masonry buildings and churches located in neighboring regions. Data on Brazilian, pure shear, indirect tensile and vertical compression tests on masonry wallettes were made fully available to the authors from previous experimental campaigns conducted by other authors; a synopsis of these results is available to the reader in [28], whereas full experimental data were available to the authors by unpublished data sets.

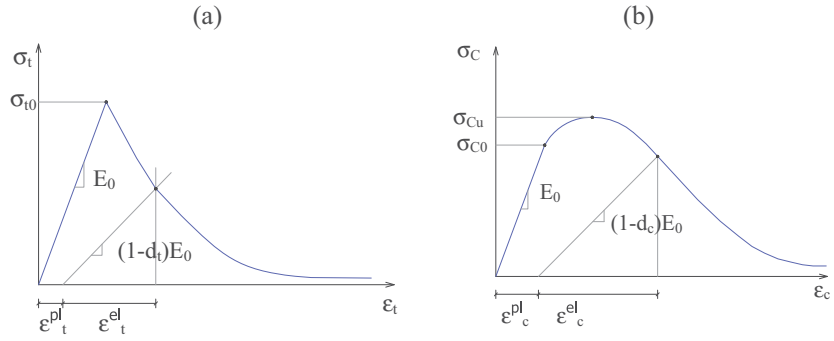

Fig. 7. Representation of the masonry constitutive behavior in (a) tension and (b) compression.

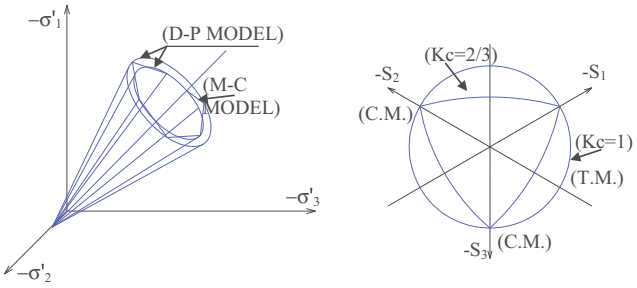

Fig. 8. ABAQUS modified Drucker–Prager strength domain.

Table 3
Main modeling parameters adopted in the simulations for masonry with the CDP in ABAQUS.

Symbol	Name	Description	Default value
Concrete Damaged Plasticity (CDP) parameters			
ϵ	Eccentricity	Distance between the points of intersection with the p-axis of the cone and the hyperbola (in the p–q plane)	0.1
f_{b0}/f_{c0}	Strength ratio	Ratio between the biaxial and uniaxial compression strength	1.16
ψ	Dilatancy angle	Angle due to a variation in volume of the material following the application of a shear force	10°
K_c	–	Ratio between distance from the hydrostatic axis of the maximum compression and traction respectively	0.666
–	Viscosity parameter	Numerical parameter which allows to reach convergence in softening without affecting the accuracy of the results	–[a]

[a] There is no default value for this parameter, since it depends on the increments value during each step; for the following analyses it has been set equal to 0.002.

It is worth noting that historical masonry is usually characterized by lack of standardization and its strength is highly influenced by local building practices and by the available raw materials. Therefore, the utilization of mechanical properties deduced from experimental campaigns conducted on coeval buildings may be, in general, questionable.

Such conclusion does not hold in this case, because the technical report prepared in 2009 by the structural engineers responsible for the restoration of the South-East wall, indicates for the existing masonry of the castle a compressive strength equal to 1.22 MPa. Such value is deduced from flat-jack tests conducted directly on the structure.

Despite such technical report is official and at disposal to the local community, it is hardly available to international readers. This notwithstanding, stress–strain behavior of the masonry mate-rial belonging to Pomposa Abbey [28] turned out to be very similar to that deduced for the castle in occasion of the 2009 restoration.

Furthermore, it appears interesting to point out that Middle-Age masonries in the area stricken by the 2012 seismic sequence seem to exhibit a quite constant (low) strength. Borri and co-workers [29], for instance, highlight how, after proper mechanical characterization done by means of different in-situ flat jack tests on several coeval buildings, masonries in such area systematically show strengths lower than those suggested by the Italian code. Degradation of mortars may be an explanation of the results obtained.

It is finally interesting to point out that the Italian Code (Testo Unico, 2008 and Circolare Esplicativa, 2009 [1,2]) in §C8A.1.A.4. recommends to adopt for existing masonry buildings made by clay bricks and lime mortar, with a low knowledge level (LC1), an average masonry compressive strength equal to 2.4 MPa. When dealing with pushover analyses, the norm requires to further reduce such value by the confidence factor, which is equal to 1.35 for a LC1. The resultant compressive strength to adopt would be slightly higher, but Italian Code does not make specific reference to the real situation found in that area.

To further corroborate the idea to adopt a lower compressive strength, it is interesting to point out that, in occasion of some surveys conducted to collect masonry triplets to test in compression in a future research, authors noticed an unusually high state of degradation of mortar in almost the totality of the unrestored castle, with joints either exhibiting almost zero resistance or being totally incoherent.

For these reasons, it was made the choice to carry out computations with values indicated by specific – but according to authors more realistic – literature values of strength for the masonry material, providing obviously lower bound estimates of the expected load carrying capacity of the structure.

Wood is used for representing the floor at the second story of the shorter arm of the Castle.

Starting from the mechanical properties adopted in the unrestored case, again in absence of comprehensive laboratory characterization of the materials to be used in a restoration, similar considerations are repeated when dealing with hypothetical properties of restored masonry.

In particular, they were evaluated by means of the results of an existing experimental campaign carried out at the Technical University of Milan, where a number of direct shear and compression tests on both improved quality lime and cement mortar restored masonry are available to the authors [30,31].

While studies [30,31] carried out by Binda and co-workers in the nineties deal again with a similar but different historical masonry (clay bricks and lime mortar), they can be reasonably assumed as representative of the expected strength increase, when

Table 4
Modal analysis results, periods of the first three meaningful modes in the different hypotheses analyzed.

T (s)	Real case		Non-restored case		Fully-restored case	
	Strand7 tetrahedral model	ABAQUS hexahedral model	Strand7 tetrahedral model	ABAQUS hexahedral model	Strand7 tetrahedral model	ABAQUS hexahedral model
Mode 1	0.394	0.398	0.398	0.403	0.318	0.322
Mode 2	0.384	0.387	0.397	0.399	0.314	0.316
Mode 3	0.381	0.383	0.383	0.385	0.304	0.306

joints are made by either improved quality lime or cement mortar. Typically, it has been found that tensile and compressive strength increase roughly by a factor 2.

On the other hand such multiplying factor to be applied on strengths appears in agreement with the Italian Code specifics, where in § C8A.1.A.4, when both good lime mortar is used and good transversal interlocking is secured a multiplying coefficient for the material resistance equal to 1.95 (1.5×1.3) can be adopted.

Finally it is worth noting that, in the expected reconstruction of the collapsed parts and in the restoration of the remaining damaged portions, it will be required, as mandatory in the technical documents reporting material specifics, the utilization of improved mortars with minimum masonry strength as in the present simulations. In such a case, the expected vulnerability reduction of the whole structure should be the one predicted here.

The low value of the Young's modulus for the infill is aimed at considering the role played by the infill itself within the seismic analysis, in such a way that both the stabilizing effect and the seismic mass are accounted for – albeit in an approximate way – without allowing for a local collapse of the vaults, which is not the object of this paper nor it occurred in reality.

As already pointed out, both the pushover and the nonlinear dynamic analyses conducted by means of ABAQUS are performed using for masonry a Concrete Damaged Plasticity (CDP) material model, already available in the standard software package, which allows for a reliable nonlinear behavior investigation of the Castle under load–unload conditions. Although the model is specifically suited for a fragile isotropic material (as is the case of concrete and not for masonry which is orthotropic [32]), its basic constitu-tive laws can be adapted for reproducing masonry properties in the inelastic range. Indeed, the "concrete model" allows for modeling materials with distinct tensile and compressive strength, as the case of masonry, with distinct damage parameters in tension and compression.

Also, the post-peak constitutive law for the material has to be defined. For both compression and tension the post-peak behavior follows a softening rule, whose decaying is faster for tension than compression.

In any case, it is worth noting that mono-axial behaviors in tension and compression are characterized by quite high values of fracture energy, which can be hardily justified in light of the existing experimental literature in the field. While authors are fully aware of such deviation from the actual masonry behavior in softening, it should be pointed out that higher values of fracture energy allow for more robust numerical stability and reduction of processing times, both necessary in this case where the number of finite elements employed is extremely high.

The CDP model [27,33] is based on the assumption of distinct scalar damage parameters for tension and compression and is particularly suitable for applications in which the material exhibits damage, especially under loading–unloading conditions, and therefore for dynamic analyses. A different inelastic behavior in tension and in compression can be introduced, as shown in Fig. 7.

To describe the multi-dimensional behavior in the inelastic range, masonry is assumed to obey a Drucker–Prager strength criterion with non-associated flow rule. A parameter $K_c = 2/3$, applied to the analytical expression for the Drucker–Prager surface in the principal stress space, allows distorting the surface, making it more similar to that of the Mohr–Coulomb criterion (Fig. 8) [19,27].

A value of 10° is adopted for the dilatation angle, which seems reasonable for masonry subjected to a moderate-to-low level of vertical compression. This value is in agreement with experimental evidences available in the literature [34] and previous numerical models recently adopted in different case studies [35,36]. To avoid numerical convergence issues, the tip of the conical Drucker–Prager strength domain was smoothed using a hyperbola. Software ABAQUS allows for smoothing the strength domain by means of an eccentricity parameter, which in the p–q plane represents the distance between the points of intersection with the p-axis of the cone and the hyperbola, where p represents the pressure component of the stress matrix while q represents its deviatoric component. A value of 0.1 is adopted in the simulations for this parameter. A suitable model should also take into account the ratio between the ultimate compressive strength in a biaxial stress state and that in uniaxial conditions. This ratio, typically taking similar values for concrete and masonry, was reasonably set equal to 1.16. A synopsis of the most important parameters utilized in the simulations is summarized in Table 3. Here it is worth-noting that the so-called "viscosity parameter" into ABAQUS may play a certain role into the determination of the peak base shear into pushover analyses, as well as can affect the global convergence of the algorithm into the nonlinear range. As a matter of fact, and in agreement with both authors' experience and ABAQUS User Guide suggested values, a small value of such parameter requires more time to achieve convergence and slightly reduces peak loads. A sensitivity analysis on a pushover load case is reported in Section 5.2 in order to show quantitatively how different values of viscosity parameters may play a role on the peak load evaluation.

The final stress–strain relationship in tension adopted for the dynamic analyses (Table 2) follows a linear-elastic branch up to the peak stress f_{t0} = 0.04 MPa and 0.08 MPa for the non-restored and restored masonries, respectively. Then, micro-cracks start to propagate within the material leading to a macroscopic softening. In compression (Fig. 7b), the response is linear up to the yield stress f_{c0} = 1.22 MPa and 2.4 MPa, again for the non-restored and restored masonries. Then, a simplified softening branch is assumed as in Table 2. The damage variables in tension (index "t") and compression (index "c") are defined by means of the following standard relations:

$$\sigma_t = (1 - d_t)E_0(\varepsilon_t - \varepsilon_t^{pl}) \quad (1)$$

$$\sigma_c = (1 - d_c)E_0(\varepsilon_c - \varepsilon_c^{pl}) \quad (2)$$

where σ_t, σ_c = uniaxial stresses; E_0 = initial elastic modulus; ε_t, ε_c = uniaxial total strains; ε_t^{pl}, ε_c^{pl} = equivalent plastic strains; and, finally, d_t, d_c = damage parameters.

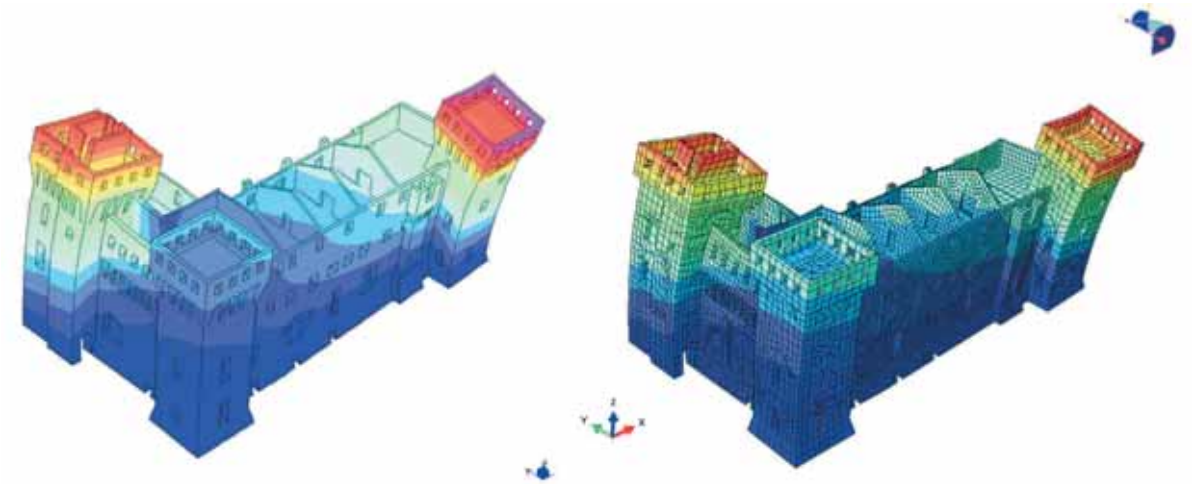

Strand 7 – Mode 1: T = 0.394 s	ABAQUS – Mode 1: T = 0.398 s
MAC = 0.983	

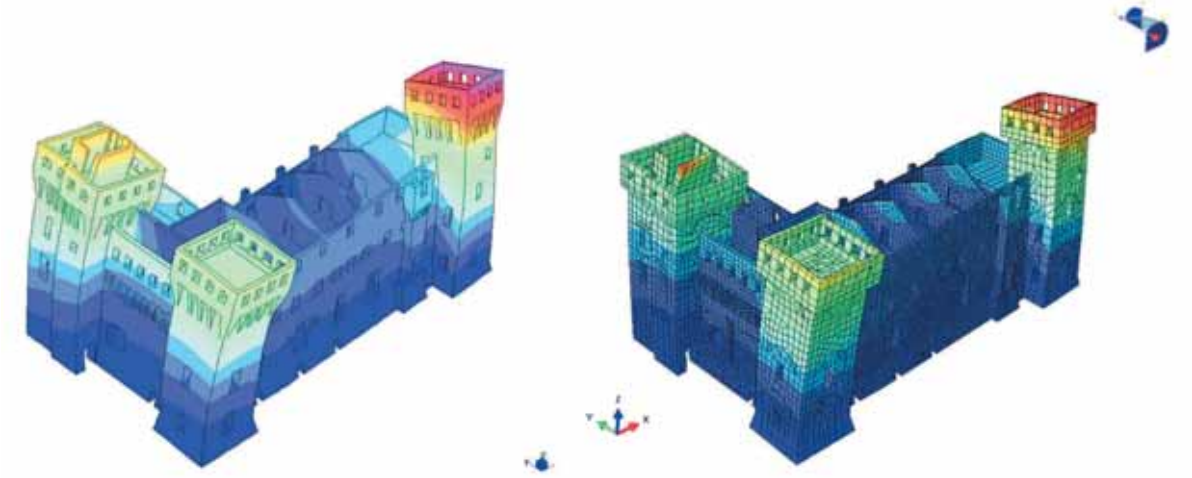

Strand 7 – Mode 2: T = 0.384 s	ABAQUS – Mode 2: T = 0.387 s
MAC = 0.976	

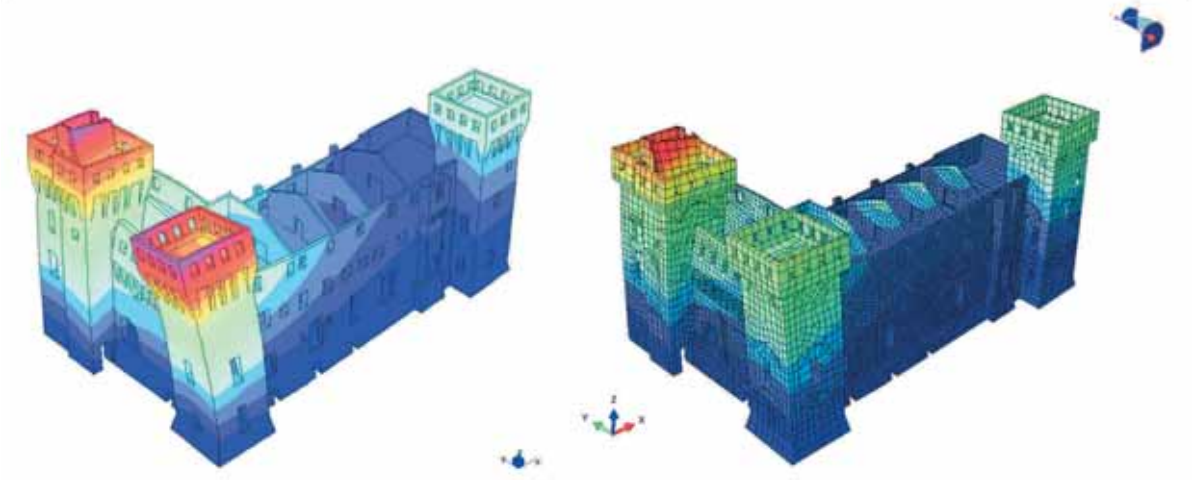

Strand 7 – Mode 3: T = 0.381 s	ABAQUS – Mode 3: T = 0.383 s
MAC = 0.909	

Fig. 9. Modal analysis for the real case.

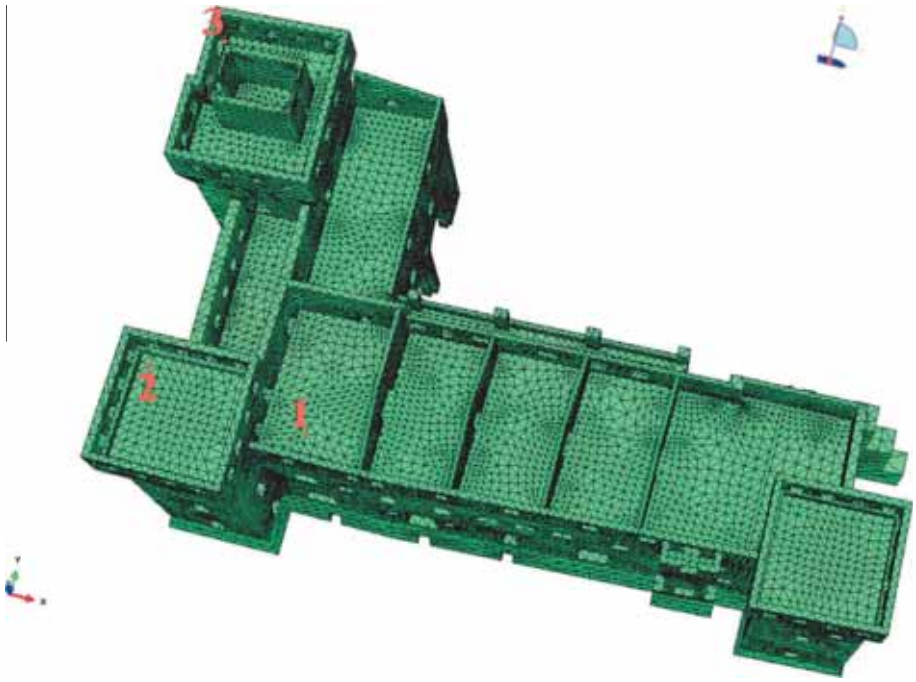

Fig. 10. Control points for the pushover analysis: second story floor (1), South Tower crown (2) and West Tower crown (3).

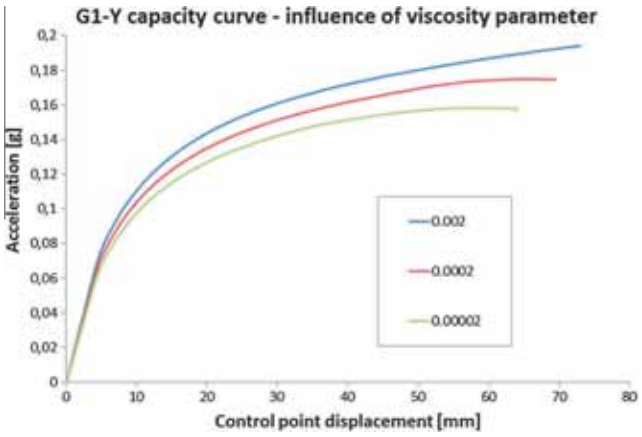

Fig. 11. Influence of viscosity parameter on a capacity curve: the value is respectively set equal to 0.002 (blue), 0.0002 (red) and 0.00002 (green). (For interpretation of the references to color in this figure legend, the reader is referred to the web version of this article.)

4. Loads applied

Loads applied to the structure depend on the typology of analysis performed. Apart modal analyses, where the issue is trivial, pushover requires the preliminary application of vertical loads, usually by means of multiple steps due to the formation of cracks in masonry elements under self-weight, and the subsequent application of horizontal loads, up to the formation of a failure mechanism. Nonlinear dynamic analyses require the application of vertical loads in the same way followed for pushover and the subsequent application of an accelerogram. In this case, a real accelerogram registered on 20th May 2012 in Mirandola (a town in the seismic crater very near to the Castle) is considered, applying to the model N–S and W–E components of the real accelerogram. As usually done for such kind of structures, the vertical component is disregarded, that however may become important for slender masonry towers. As far as pushover analysis is concerned, [4] suggests the evaluation of the load carrying capacity by means of two configurations of horizontal forces: the first is a distribution of forces derived by the assumption of a linear variation of

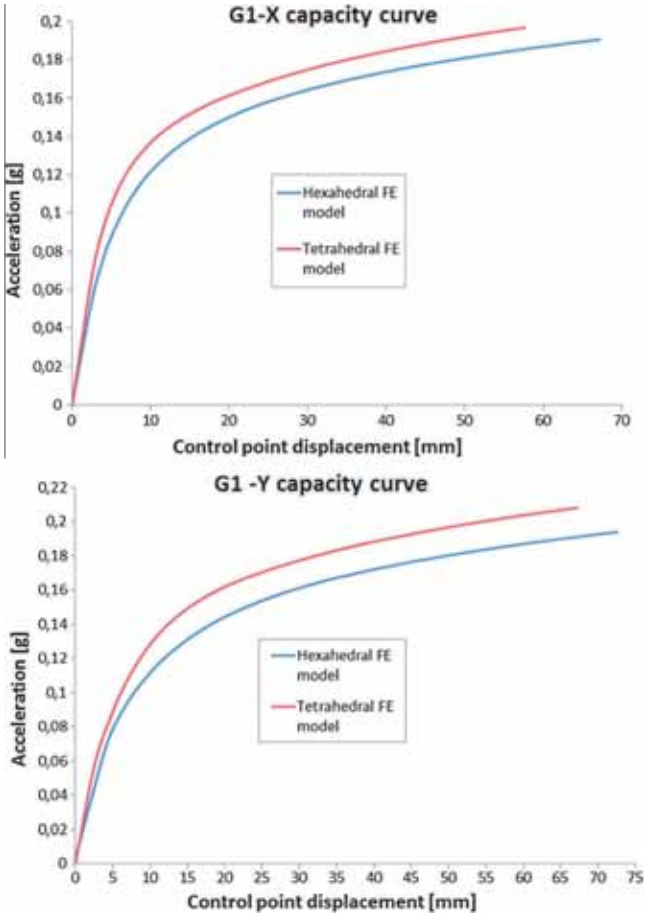

Fig. 12. Hexahedral vs tetrahedral FE model (point 1).

acceleration along the height (roughly corresponding to the first distribution of Group 1 in [1], or G1) while for the second it is assumed a constant acceleration (the first of Group 2 in [1], or G2). As prescribed by [2], the first distribution of forces of Group 1 and Group 2 can be applied independently of the participating mass activated by the first mode. Since the Castle shape is not sym-metric by any means, pushover analyses should be performed for all the possible configurations of horizontal loads (8 overall), how-ever a preliminary set of analyses revealed that the most affecting configurations for the structure are G1-X and G1-Y, therefore only these two distributions will be taken into account from now on.

As already pointed out, the seismic response of the Castle under three different hypotheses for the material is investigated:

(1) "Real case", i.e. the case corresponding to the actual situation of the Castle at the occurrence of the 2012 earthquake.
(2) "Non-restored case", i.e. the case corresponding to the situation of the Castle before the 2009 renovation, in which the main façade masonry shares the same non-restored material properties of the remaining part of the structure.
(3) "Fully-restored case", i.e. a hypothetical situation in which the 2009 renovation is supposed extended to the whole structure, so that the masonry of the Castle is restored everywhere.

5. Numerical results

In absence of indications by [4] regarding simplified safety assessments applicable to complex structures as castles, the numerical simulations performed in the paper rely into preliminary modal, nonlinear static and dynamic analyses.

Preliminary modal analyses are carried out in order to have an insight into the performance of the coarse hexahedral mesh (Mesh 2) when compared with the refined tetrahedral one (Mesh 1) in reproducing with a certain accuracy eigen-frequencies and eigen-modes of the fundamental vibration modes. Pushover and nonlinear dynamic analyses represent the core of the research carried out and have the final aim to have an insight into the response of the structure if assumed totally or partially restored. In addition, nonlinear dynamic simulations allow to put in evidence pros and cons of pushover.

5.1. Modal analyses

In terms of modal analysis, it is possible to make a comparison among the three cases for both the tetrahedral model in Strand7 and the hexahedral model in ABAQUS. The results for the first three principal modes of the structure show quite similar values in terms of periods and a very good correspondence in terms of modal shapes for each case; moreover, the "non-restored case" shows slightly higher values of the periods – which corresponds to a slightly lower stiffness for the structure – while the "fully-restored case" shows the very opposite (lower values of the peri-ods, i.e. higher stiffness for the structure).

A synopsis of the periods found within Strand7 and ABAQUS in the three different cases is reported in Table 4, whereas the modal deformed shapes – albeit only for the real case in order to avoid redundancy – are depicted in Fig. 9, where also a quantitative comparison is shown in terms of Modal Assurance Criterion (MAC), with a procedure fully described in [37], by picking 24 relevant points on different levels on the towers and on the main body.

From a numerical standpoint, a rather satisfactory agreement between results found with Mesh 1 and Mesh 2 can be observed, both in terms of period values and modal deformed shapes, meaning that Mesh 2 may be regarded as a good compromise to perform sufficiently reliable analyses with a reduced computational effort.

As can be seen from a detailed comparison among all results, in agreement with intuition, the differences between real case and non-restored case are minimal, because the only variation of stiffness is concentrated on one of the external walls. The fully restored models are obviously stiffer and provide smaller periods (differences of around 20%). The deformed shapes are quite global, with the clear activation of the masses concentrated on all towers. Intuitively, such an output may suggest that partial collapses in correspondence of towers crowns are more likely. Moreover, the modal deformed shapes are arguably affected by the structural irregularity which characterizes the castle: in fact, the towers show light torsional effects in all three modes, whereas the main body exhibits a rather regular behavior thanks to the squat geometry and the stiffening effects induced by the towers themselves. Also, the comparison in terms of MAC shows a good correspondence between the modal shapes of Mesh 1 and Mesh 2 for each mode, with a degree of consistency always higher than 90% for the three modes considered.

5.2. 3D pushover analyses

The so-called pushover is a nonlinear static procedure generally used to determine the structural behavior against horizontal forces or displacements applied.

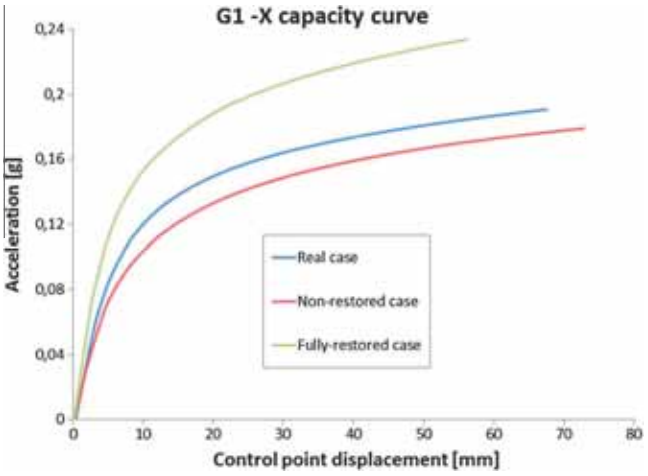

Fig. 13. G1-X capacity curve for the three cases (point 1, Mesh 2).

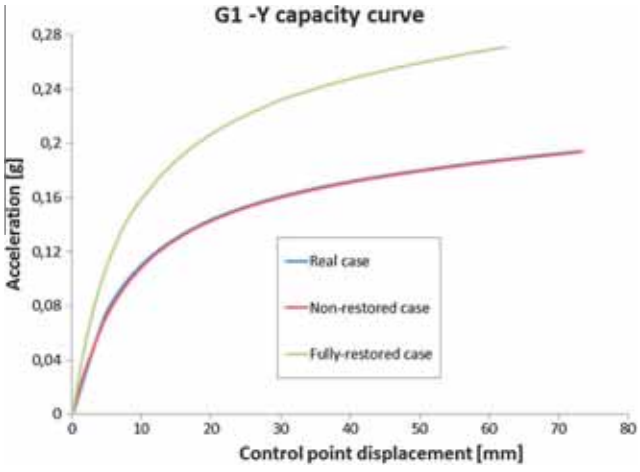

Fig. 14. G1-Y capacity curve for the three cases (point 1, Mesh 2).

This is a simplified procedure adopted in the last few years also for the nonlinear static analysis of masonry structures, see e.g. [38]. Basically, a computational model of the structure is loaded with a proper distribution of horizontal static forces, which are gradually increased with the aim of "pushing" the structure into the nonlinear field. The resulting response conveniently represents the envelope of all the possible structural responses, and can be thus used to replace full nonlinear dynamic analyses. Here full 3D pushover analyses are performed on the 3D models previously described.

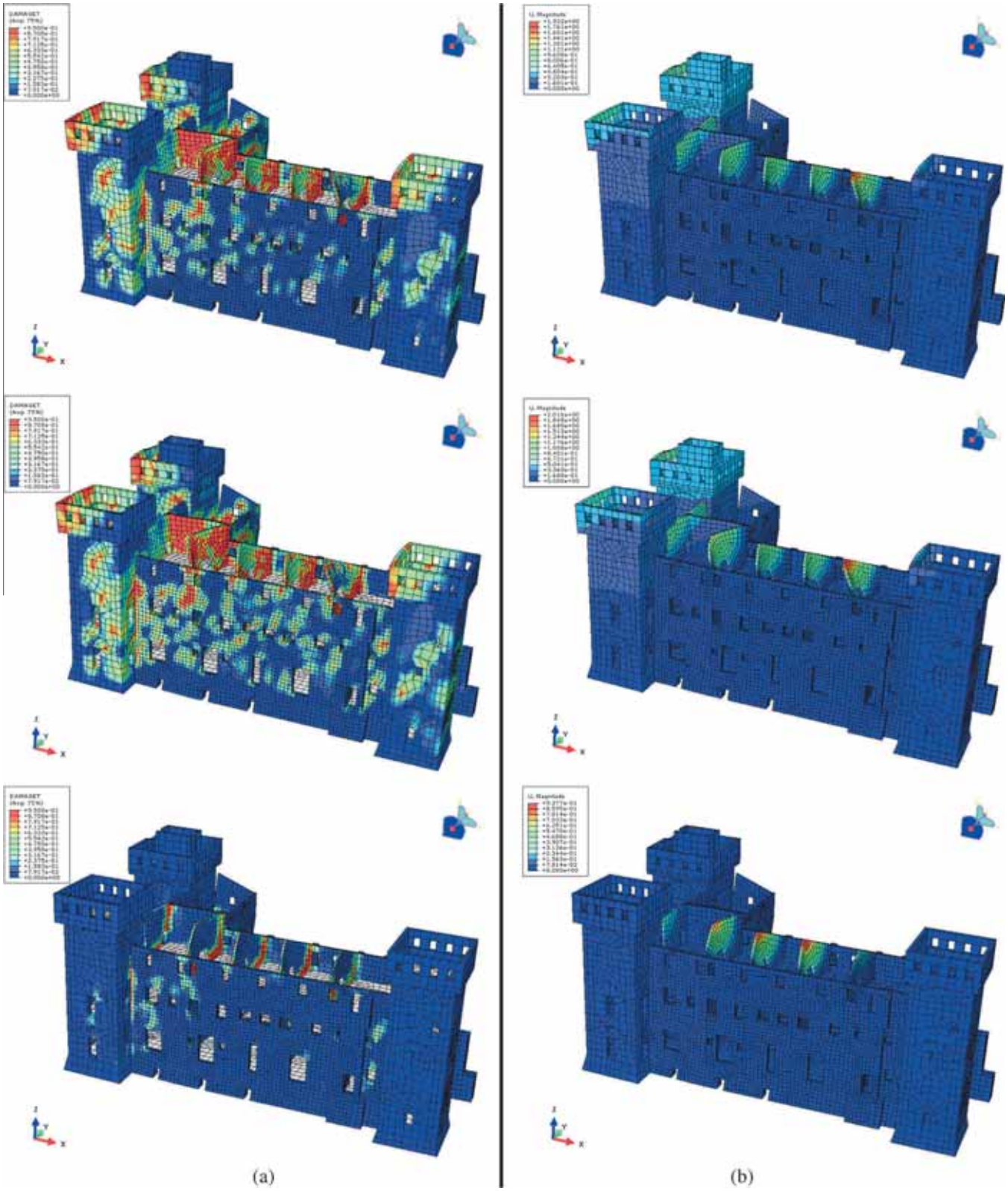

Fig. 15. (a) Damage and (b) displacement maps for G1-X at performance point displacement: real case (top), non-restored case (middle), fully-restored case (bottom).

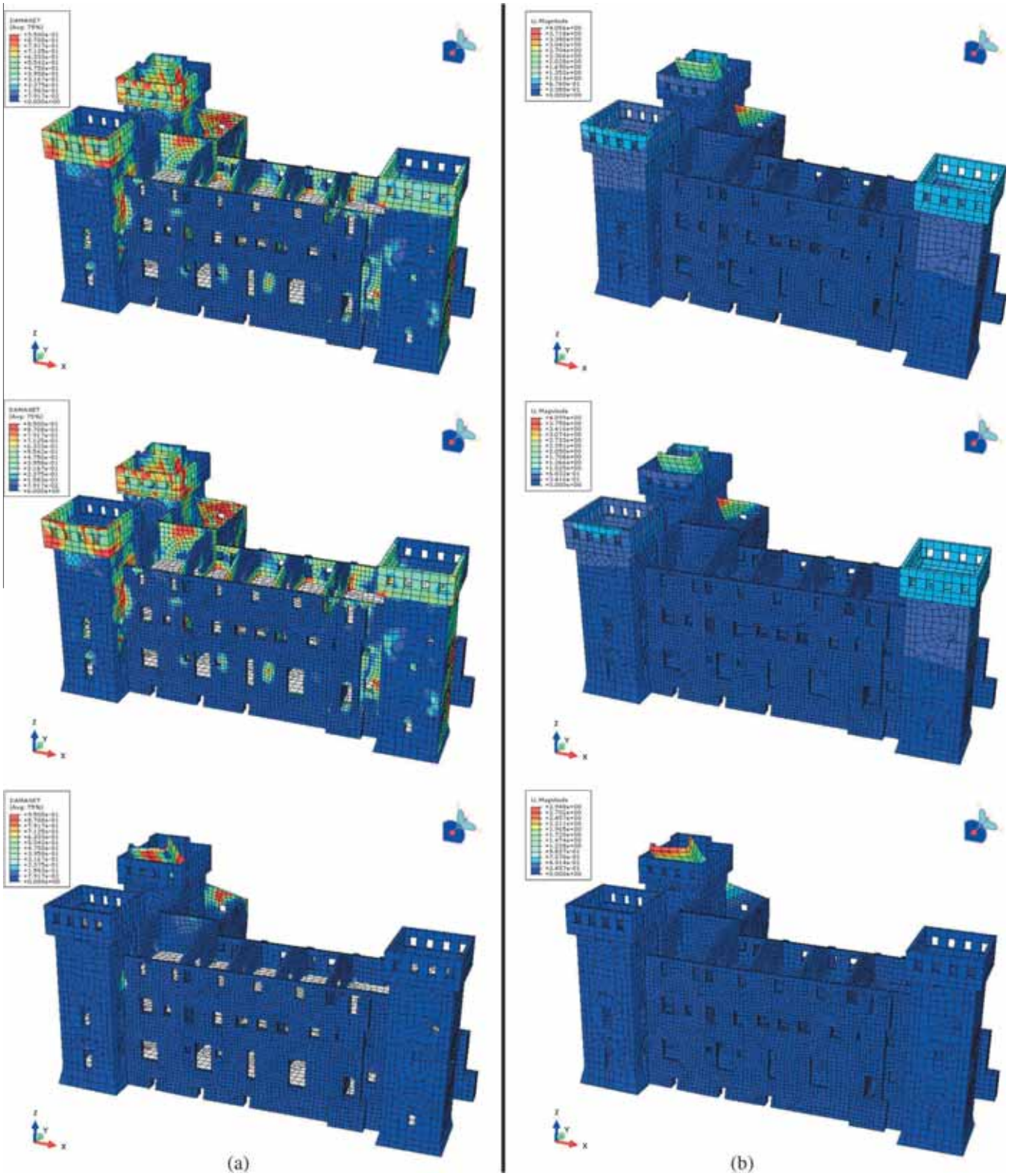

Fig. 16. (a) Damage and (b) displacement maps for G1-Y at performance point displacement: real case (top), non-restored case (middle), fully-restored case (bottom).

The choice of the control point for the pushover analyses of historical masonries is clearly a controversial issue [39], because the behavior is rarely global [5,8,12]. Generally, in presence of active partial failure mechanisms, the control point should belong to the collapsing macro-block. In the present paper, however, the behavior of the Castle, exception made for towers crowns and some walls of minor importance may be regarded as quite global. For this reason, the choice of the control point is less critical. In agreement with standard pushover on ordinary buildings, the point has been taken in correspondence of the second story floor level, as indicated in Fig. 10 (point 1). In the real case, however, col-lapse of the upper part of one of the towers is experienced. For this

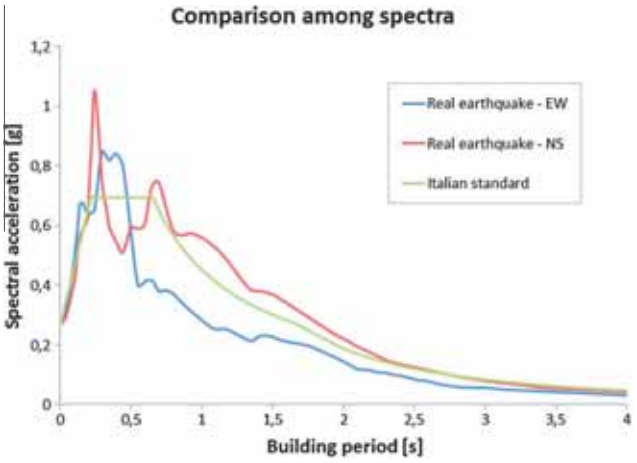

Fig. 17. Comparison among different spectra: spectra obtained for the real earthquake in the East–West (blue) and North–South (red) directions, and spectrum proposed by the Italian standard (green). (For interpretation of the references to color in this figure legend, the reader is referred to the web version of this article.)

reason, when dealing with N2 safety assessment, two further control points are monitored, one on the South Tower crown and one on the West Tower crown (respectively, points 2 and 3 in Fig. 10), the latter with the aim of investigating if the partial collapse of the tower crown can be predicted within a displacement based approach and a global pushover analysis. Further considerations on the matter will be done in the following section.

The same CDP model utilized for the nonlinear dynamic analyses is used for pushover simulations. While in the model damages in both tension and compression are possible, global pushover curves rarely exhibit any visible softening. This is almost always linked to the negligible active damage in compression and the very low fracture energies in tension. As a matter of fact, the global behavior is intrinsically ruled by masonry self-weight and the contribution of the limited tensile strength on the overall horizontal capacity is almost always negligible. Such a typical behavior does not allow, in principle, the reduction to a 1DOF elasto-plastic system to perform displacement based safety assessments. This notwithstanding, such behavior is well known and expected of complex 3D masonry models. For such a reason, [4] allows the reduction to a 1DOF system even without any visible softening of global pushover curve, with a procedure fully described in [19], where the interested reader is referred to.

As already pointed out in Section 3, the choice of the viscosity parameter may play a certain role in non-linear static analysis, leading to an overestimation of the peak base shear for high values of the viscosity parameter. In order to have a quantitative insight into such issue for the case study under consideration, a sensitivity analysis has been carried out by the authors changing the viscosity parameter in a wide range when determining the nonlinear static behavior of the Castle under a certain distribution of horizontal loads (namely G1) along one of the geometric directions of the structure. Authors experienced a slight overestimation of the collapse base shear when using high viscosity parameters (not recommended theoretically but used to speed up nonlinear computations), which however falls within engineering practice acceptability. An example is provided in Fig. 11 for the sake of clearness.

Preliminarily and once calibrated a viscosity parameter value representing a compromise between reliability of the results and computational efficiency, when dealing with the real case, a comparison between resultant pushover curves from the tetrahedral and the hexahedral models is provided. The results, depicted in Fig. 12, show that the capacity curve for the tetrahedral model is slightly higher than the one for the hexahedral model, meaning that the former is mildly stiffer and more resistant than the latter, a result fully in agreement with the FE formulation of the two models (i.e. the inherent higher stiffness of the tetrahedral one). Pushover curves are provided as horizontal acceleration a_g normalized against gravity acceleration vs control node horizontal displacement.

As can be seen, the difference between pushover curves provided by the two models is lower than 10% in the most unfavorable case, a result fully acceptable from an engineering standpoint, which allows the utilization of both models to perform nonlinear static analyses.

Once established the satisfactory agreement between results provided by the two meshes, it is possible to make a comparison among the three cases (real, non-restored, fully-restored) for both distributions of horizontal loads:

– For G1-X case, see Fig. 13, the results show that the capacity curve for the non-restored case is beneath the one for the real case, whereas the capacity curve for the fully-restored case is consistently higher. This means that the 2009 renovation has

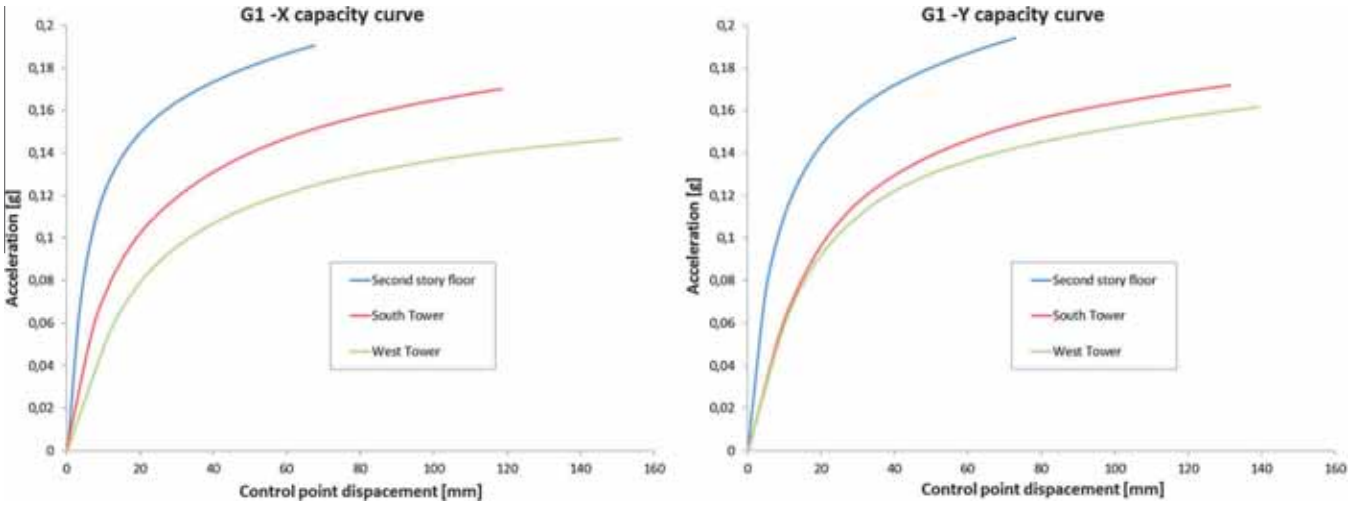

Fig. 18. Pushover capacity curves obtained with different control points (Mesh 2).

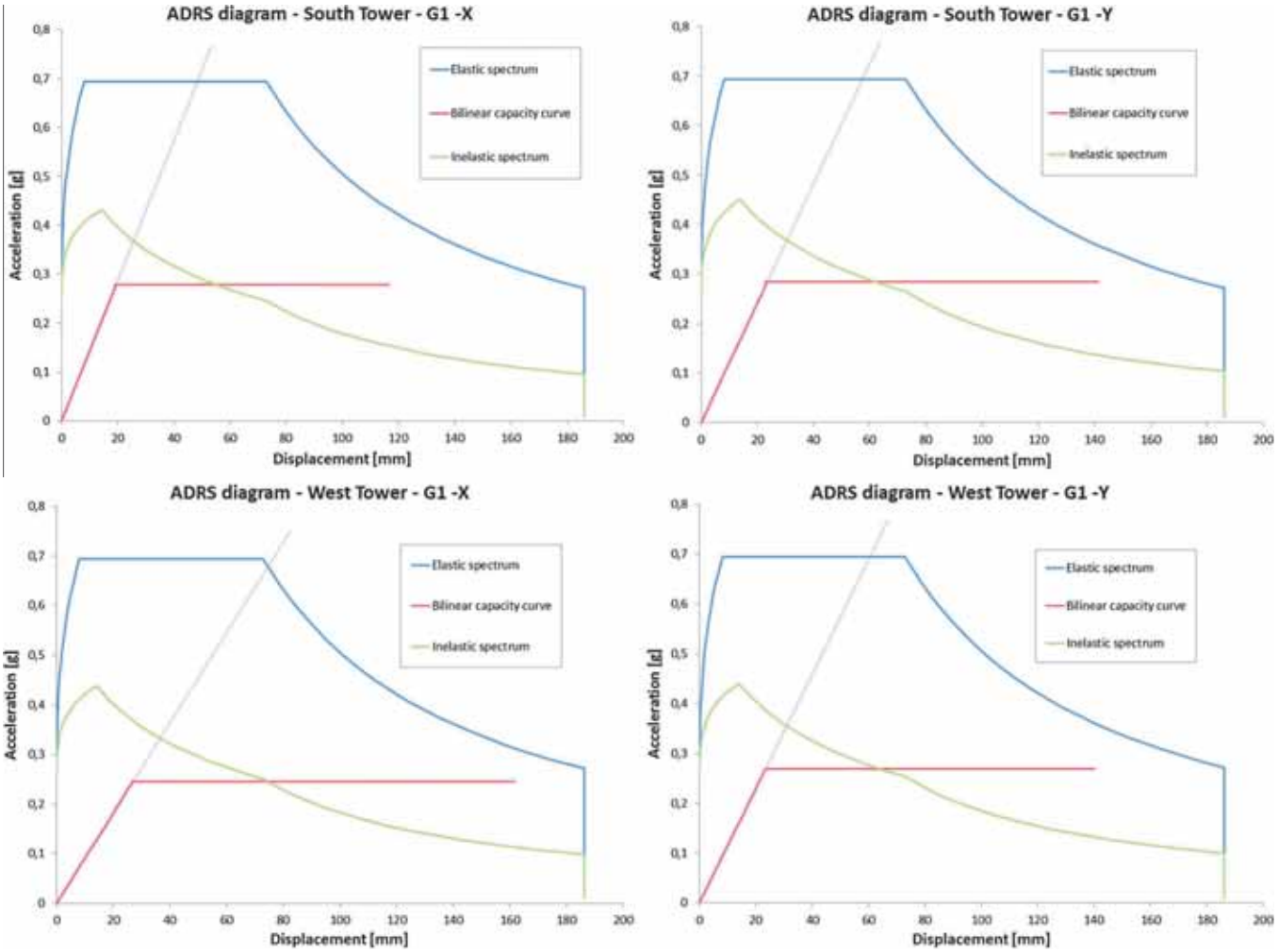

Fig. 19. Safety assessments for the two control points on the towers crown done with the N2 method.

Table 5
Parameters for the N2 method for the two control points on the towers crown.

		Displacement demand d^*_t (mm)	Displacement capacity d^*_u (mm)	Verified
N2 method – parameters				
South Tower crown (point 2)	G1-X	55.0	116.5	YES
	G1-Y	61.7	141.3	YES
West Tower crown (point 3)	G1-X	74.6	161.7	YES
	G1-Y	64.0	140.4	YES

actually increased both the stiffness and the strength of the Castle along this direction – which is obvious since the main façade itself is located along the direction of application of the load. If the renovation had been extended to the whole building, the global resistance would have further increased, probably precluding the observed damages.

– For G1-Y case, see Fig. 14, the results show that the capacity curve for the non-restored case is almost superimposable with that obtained for the real case, while the capacity curve of the fully-restored case is far above. This means that the 2009 renovation has not had any effect on the stiffness of the Castle along this direction, while the extension of the renovation to the whole building would have considerably increased the load carrying capacity and the initial stiffness. This is not surprising because the restored wall is oriented along the *X* direction and its contribution on the global strength of the structure when loaded out-of-plane (i.e. for *Y* direction) is negligible.

The aforementioned results are further confirmed by making a comparison in terms of damage and displacement maps for the three cases, see Figs. 15 and 16:

– For G1-X case, Fig. 15, the damage map for the non-restored case shows the presence of a more diffused damage on the main façade (i.e. that subjected to the 2009 restoration) with respect to the one for real case. Damage map for the fully-restored case shows a remarkable reduction of damages for the whole structures, and also different damaging mechanisms with respect to

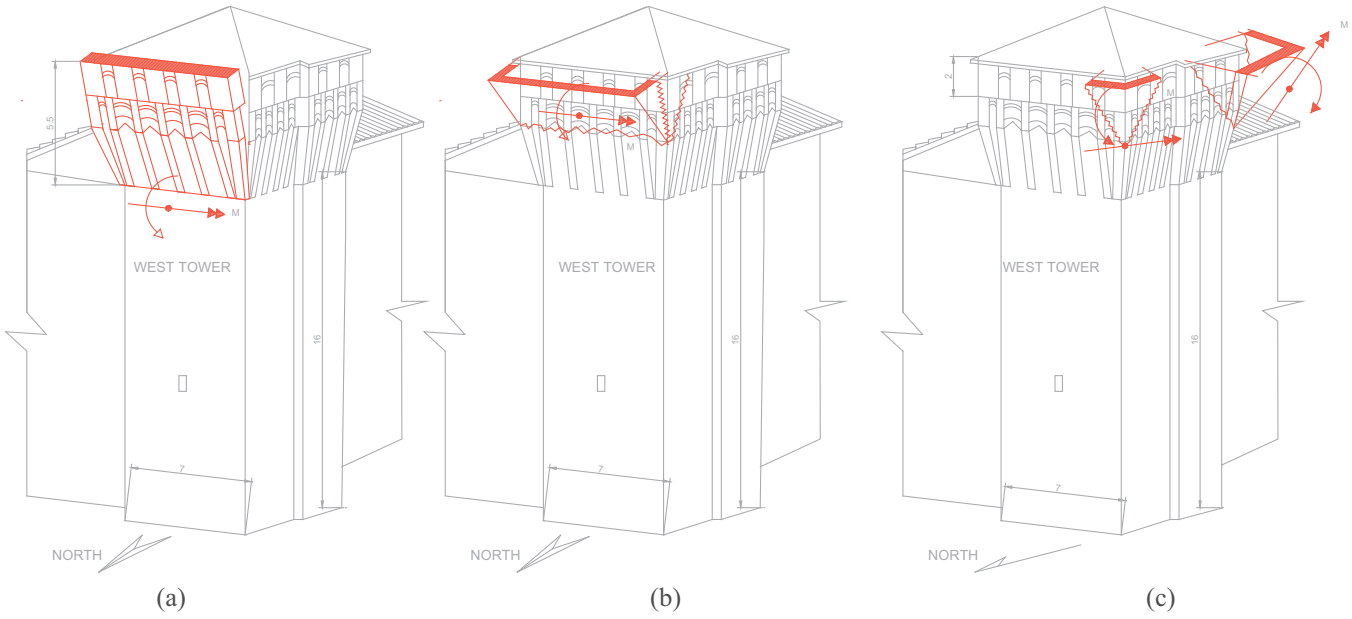

Fig. 20. Failure mechanisms: from left to right, simple out-of-plane overturning (a), composite out-of-plane overturning (b) and corner out-of-plane overturning (c).

Table 6
Comparison between the rocking failure collapse accelerations for the three towers and the accelerations related to the earthquake.

Failure mechanism	Collapse acceleration (g)	Spectrum peak acceleration (g)	Check	Earthquake mean acceleration (g)	Check
Simple out-of-plane overturning – East and South Towers	0.244	0.231	YES	0.200	YES
Simple out-of-plane overturning – West Tower	0.073		NO		NO
Composite out-of-plane overturning – East and South Towers	0.250		YES		YES
Composite out-of-plane overturning – West Tower	0.094		NO		NO
Corner out-of-plane overturning – East and South Towers	0.334		YES		YES
Corner out-of-plane overturning – West Tower	0.172		NO		NO

the real case; the displacement maps obtained at the end of the simulations for the three cases confirm what previously pointed out on the role played by a diffused restoration.

– As expected, for G1-Y case, see Fig. 16, the damage map for the non-restored case shows no actual difference with respect to the one obtained for the real case. This is in agreement with the negligible role played by the restored wall (loaded out-of-plane) in the global strength increase of the structure. Consistently, the damage map obtained for the fully-restored case shows similar features when compared with that obtained in the G1-X case, i.e. high reduction of damaged zones, different damaging mechanisms with respect to the real case, reduction of the global vulnerability of the structure.

5.3. N2 method safety assessment

For the pushover analyses of the real case, where partial failure mechanisms are experienced, a specific study is performed in terms of the choice of the control point: the goal is to verify if a proper choice would have forecast the structural weakness in the upper part of the towers, on which diffused damages occurred along with the partial collapse of the West Tower. The check has been made with the N2 method according to [3,40], investigating three different control points, as illustrated in Fig. 10: one on the second story floor, one on the crown of the West Tower (point 3 in Fig. 10), and a further control point located on the South Tower (point 2 in Fig. 10) checked for the sake of completeness. The elastic spectrum used for the N2 method is the one provided by the Italian standard for the site of Finale Emilia, as one would expect due to the a priori nature of the method itself; the Italian standard spectrum is also compatible with the real spectra obtained for the considered earthquake, as shown in Fig. 17. The results, summarized in Fig. 18, show that the capacity curve of each point lies beneath the one for the control point on the second story floor (so in those points the structure is far less stiff), with a greatly higher value of the ultimate displacement for the structure. Nonetheless, the check done by means of the N2 method is positive for both points located on the towers (Fig. 19 and Table 5); this means that the pushover analysis is not able to forecast the insur-gence of local effects, indeed it allows only global checks of the structure.

5.4. Limit analyses

Some limit analyses were performed on three pre-assigned failure mechanisms on the towers, namely simple out-of-plane overturning, composite out-of-plane overturning and corner out-of-plane overturning (see Fig. 20). These three mechanisms were considered for all the towers (in Fig. 20 those relevant for the most damaged are shown), and their corresponding collapse accelerations were compared to the peak acceleration related to the spectrum provided by the Italian standard and the mean acceleration for the real earthquake. The results are presented in Table 6. The choice of such failure mechanisms instead of others is obviously

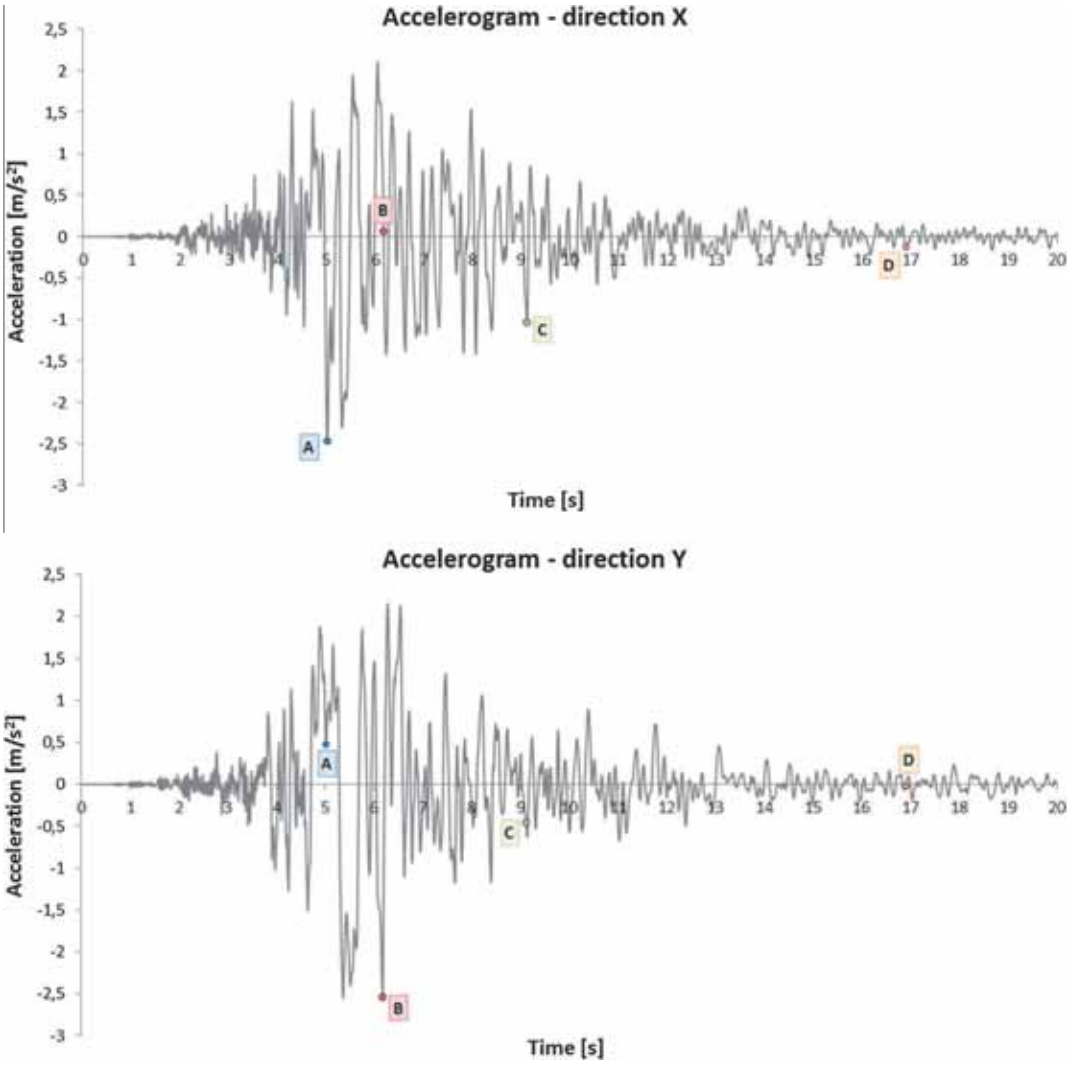

Fig. 21. Real accelerograms used in the non-linear dynamic analyses.

inspired by the real collapses observed especially on the upper part of the West tower, but also on the East tower. Sketches reported in Fig. 20 correspond precisely to the blocks forming the failure mechanism considered to evaluate the collapse accelerations reported in Table 6. By means of the application of the kinematic theorem of limit analysis on such mechanisms and assuming the masonry material as unable to withstand tensile stresses, it is very straightforward – for instance by means of a commercial spreadsheet – to estimate the horizontal acceleration associated to the activation of such mechanism. Vertical loads acting are masonry self weight and dead loads of the roof and the floors, when involved in the failure mechanism.

As can be observed, the limit analyses show a good correspondence to what occurred in reality: rocking failure mechanisms had indeed activated on the upper part of the West Tower (Fig. 3a and b), while the East and South Towers had been spared, although the simple and composite out-of-plane overturning mechanisms present collapse accelerations which are fairly close to the ones related to the earthquake, and this helps explaining the cracks on the other towers (Fig. 3c).

5.5. 3D nonlinear dynamic analyses

The nonlinear dynamic analyses are performed by means of the application of N–S and W–E components of a real accelerogram registered in occasion of the first main shock on May 20th, and recorded in the nearby town of Mirandola.

Four meaningful instants of the analysis are considered in detail and identified in the accelerograms with different letters and colors, see Fig. 21. The chosen instants are the following:

- Instant A (blue[1]): absolute acceleration peak along X direction.
- Instant B (red): absolute acceleration peak along Y direction.
- Instant C (green): half time of the recorded ground motion.
- Instant D (orange): practical end of the seismic excitation.

By means of the damage development sequence shown at the different instants, it is possible to have a deep insight into the formation of the damage mechanisms. In addition, it is possible to plot the displacement time-history for the two relevant control points, shown in Fig. 22.

From the displacement time-history of the selected nodes, it can be deduced if significant residual displacements are present at the end of the simulations. If there are considerable residual displacements, it means that large inelastic deformation occurred, which is an indication of the possible activation of failure mechanisms.

[1] For interpretation of color in Fig. 21, the reader is referred to the web version of this article.

Fig. 22. Control points for the nonlinear dynamic analysis: main façade top edge (1) and West Tower crown (2).

On the other hand, relatively high fracture energies (especially in compression) were used by the authors in order to avoid premature halting of numerical analyses due to the activation of partial failure mechanisms of small portions of the structure, mainly located in the upper part of the towers. Such local failures are typically due to much reduced masonry strength in all those parts where vertical confinement is very small or totally absent. Since the object of the present investigation is to have an insight into the global behavior of the Castle, authors adopted less fragile stress–strain relationships with the aim of successfully conducting the analyses also in presence of very high displacements of limited portions of the structure (namely the upper parts of the towers), as clearly visible from the deformed shapes. In the following subsections, a discussion of the nonlinear dynamic results obtained for the three cases investigated is separately reported.

5.5.1. Real case situation

Deformed shapes of the structure at the different meaningful instants investigated are represented in Fig. 23. In the same figure, the color patches of the damage parameter D_t in tension are also represented: red color is associated to full damage ($D_t = 1$), whereas blue color to zero damage ($D_t = 0$). As can be noted from the deformed shapes and from damage contour plots at the different instants, a diffused damage develops during the application of the accelerogram on the upper part of all three towers. From a crit-ical analysis of the deformed shape and the damage map evolution, it can be stated that an active, local failure mechanism is present on the top of the West Tower, which closely represents what actu-ally occurred to the structure in the aftermath of the May 20th main shock. This is further confirmed by the horizontal displace-ment time-history diagram of the control point located on the West Tower which – after a small initial oscillation – quickly increases, reaching values suggestive of a local collapse of the upper part, see Fig. 24. The horizontal displacement diagram for the control point on the main façade shows obviously a huge oscillation in correspondence of the critical instants of the shock, whereas a residual absolute displacement of about 5 mm is present at the practical end of the simulations, which means that the main façade is in a condition very far from the ultimate limit state.

5.5.2. Non-restored case

The evolution of damage and deformed shapes of the structure at the different instants investigated is represented in Fig. 25. As expected, the trend is globally similar to the previous case, but with a conspicuous difference concentrated on the main façade, which features more diffused damages than in the real case. Once again, the top of the West Tower presents a deformed shape which clearly corresponds to a local collapse. The horizontal displacement diagram for the control point on the West Tower features again a sudden increase after a small initial oscillation, with absolute values and global trend generally almost equal to the previous case analyzed (real case hypothesis). On the contrary, the diagram on the control point located on the main façade is more irregular with respect to the one obtained for the real case. At the practical end of the simulation, a residual displacement of 25 mm is present, 5 times greater than the one experienced in the real case. This may suggest that also the upper part of the main façade is not far from the activation of a partial failure. It is therefore straightforward to conclude that the restoration done in 2009, despite partial, helped in the preservation of the portion of the Castle near the main façade (see Fig. 26).

5.5.3. Fully-restored case

A concise synopsis of the nonlinear dynamic analysis results obtained is reported in Fig. 27, where deformed shapes and tension damage parameter patch evolution are represented. In terms of damage contour plots, huge differences with respect to the two previous cases emerge: indeed, damaged zones look completely different. In particular, the upper parts of the three towers are completely free from meaningful damage, which conversely is present only on few parts of the structure. Only a small portion located on the top of the West Tower seems to exhibit a sort of minor local collapse. The horizontal displacement time-history diagram for the control point on such tower features an oscillating behavior with no sudden increase, exhibiting a residual displacement of almost

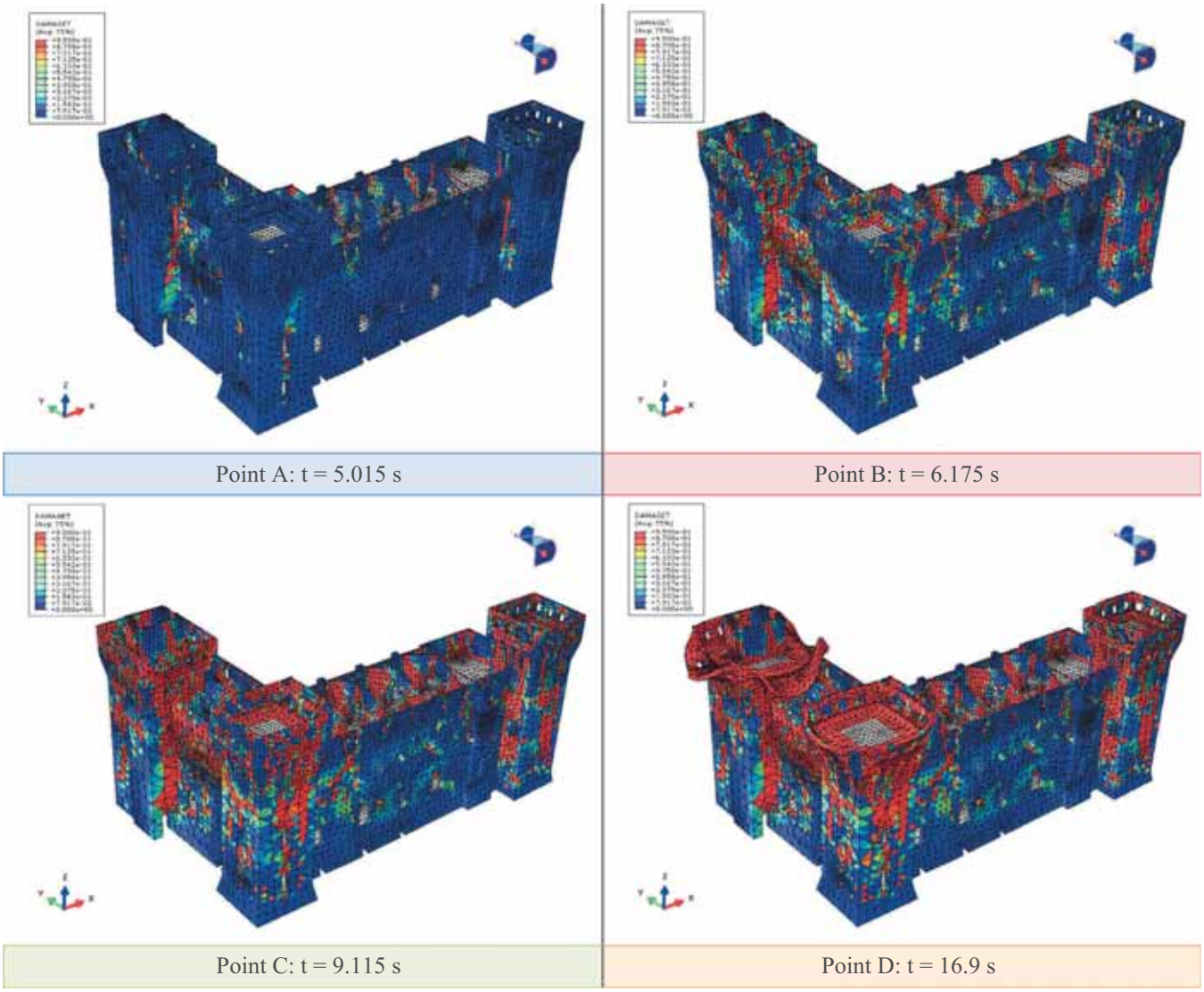

Fig. 23. Real case hypothesis. Deformed shapes with damage patch in tension at the different meaningful instants indicated in Fig. 21.

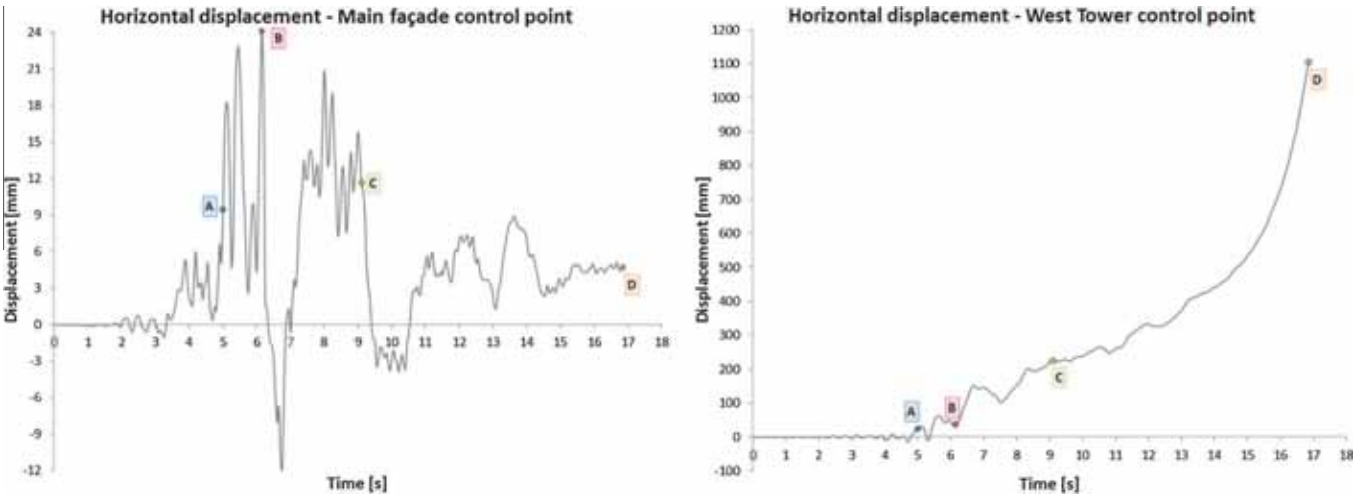

Fig. 24. Real case hypothesis. Horizontal displacement time-history diagrams for the two control points shown in Fig. 22.

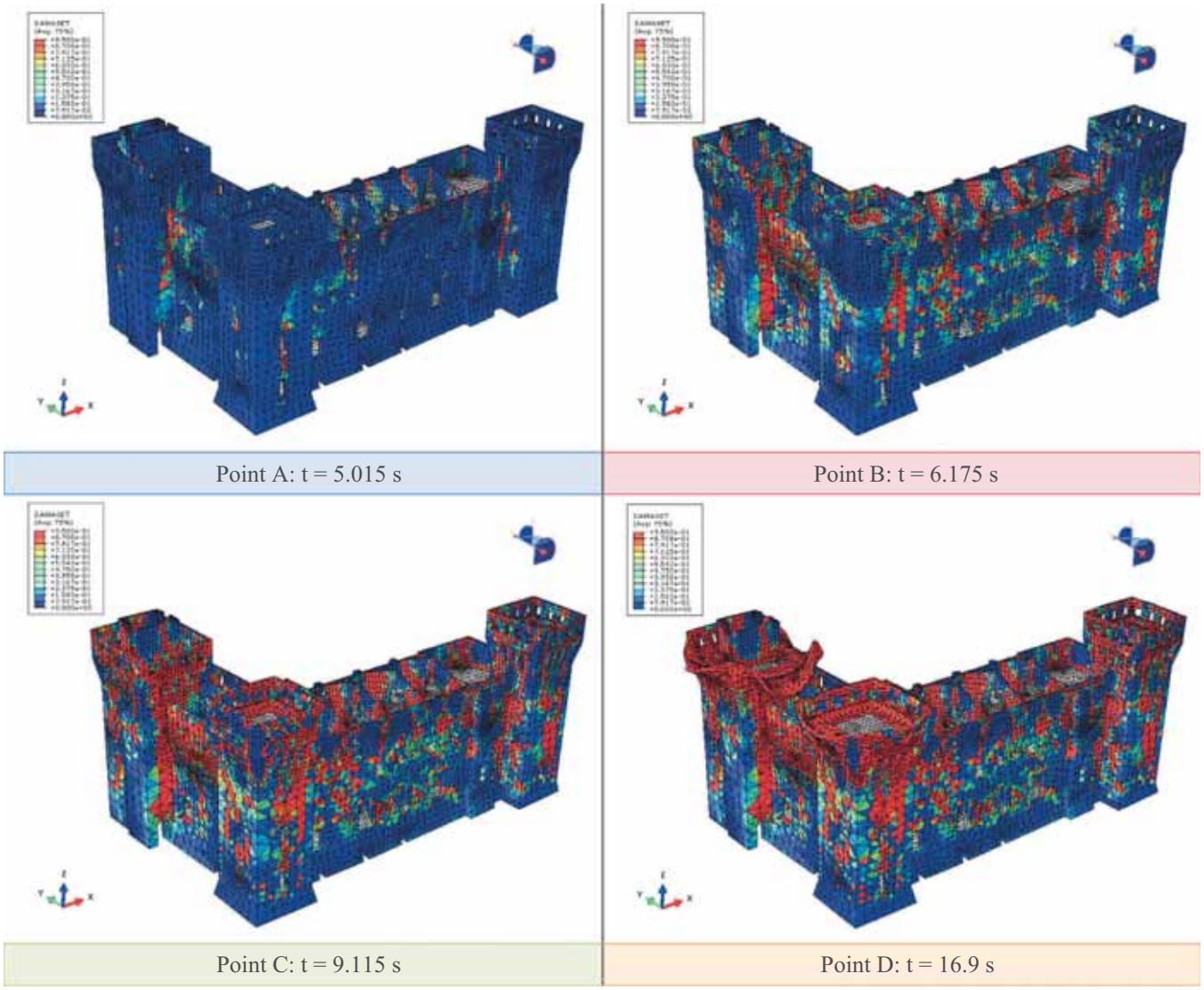

Fig. 25. Non-restored case hypothesis. Deformed shapes with damage patch in tension at the different meaningful instants indicated in Fig. 21.

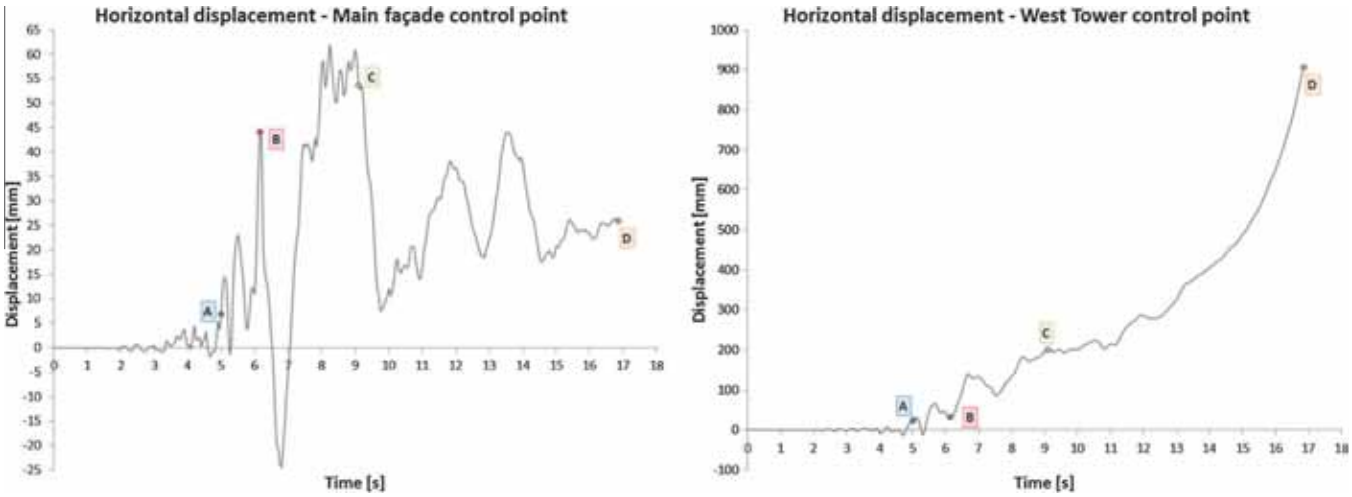

Fig. 26. Non-restored case hypothesis. Horizontal displacement time-history diagrams for the two control points shown in Fig. 22.

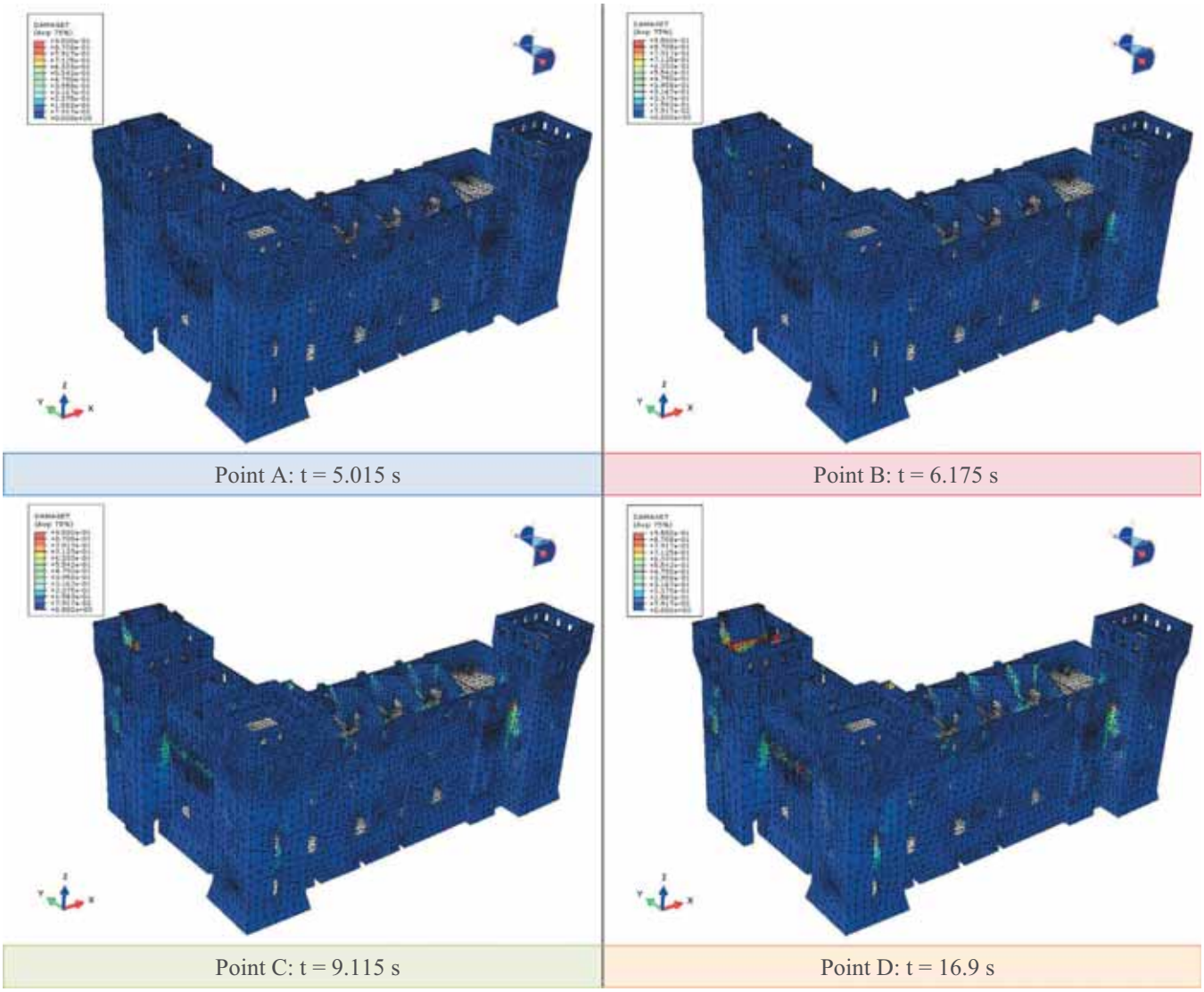

Fig. 27. Fully-restored case hypothesis. Deformed shapes with damage patch in tension at the different meaningful instants indicated in Fig. 21.

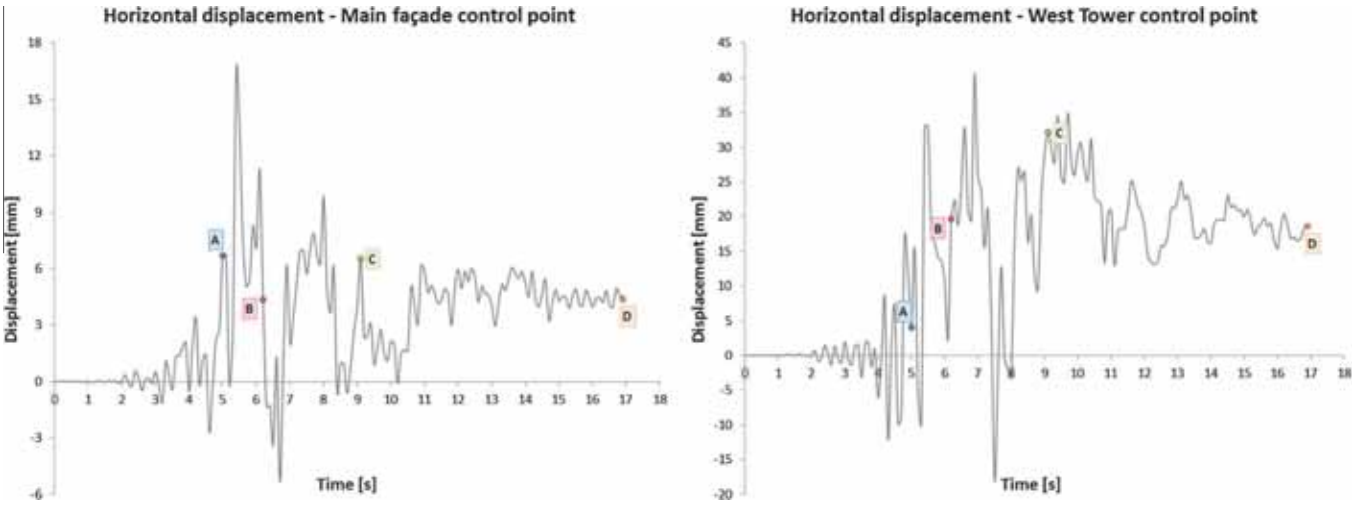

Fig. 28. Fully-restored case hypothesis. Horizontal displacement time-history diagrams for the two control points shown in Fig. 22.

20 mm, which seems still not compatible to the activation of a failure mechanism. In addition, the horizontal displacement diagram of the control point located on the main façade shows a behavior close to the one obtained for the real case, with a residual displacement of 5 mm, again far away from values compatible with a local failure, see Fig. 28.

The comparisons reported in Fig. 29 clearly show that the fully-restored case is not affected by meaningful damages and activation of local failure mechanisms. The real case situation and the non-restored case hypotheses provide quite similar results, with slight differences near the main façade, which obviously is less vulnerable if considered restored.

5.6. Discussion on the adopted parameters for the FE solver and limitations of the choices adopted

The analyses were performed using an arc-length routine available in ABAQUS (Riks algorithm), suitable to take into account possible softening exhibited by the global pushover curve, which however is never observed by the authors in the present case, due to the very low tensile strength adopted and the negligible fracture energy in tension.

Nonlinear dynamic analyses were conducted again within ABAQUS [27], which allows for a realistic reproduction of the actual masonry behavior under nonlinear load–unload conditions by using independent damage parameters in tension and compression, and a 3D behavior ruled by a regularized Drucker–Prager strength criterion, as already discussed in Section 3. The geometric

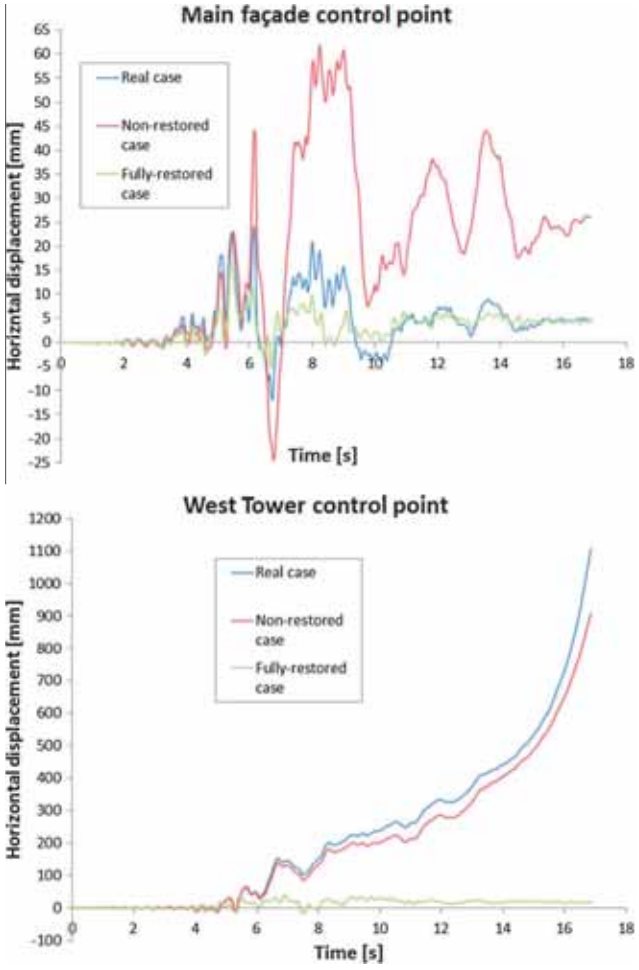

Fig. 29. Horizontal displacement for two control points in the three cases investigated.

Table 7
Computational time for each analysis.

Case	Analysis	Computational time
Real case	Pushover G1-X	19 h
	Pushover G1-Y	18 h
	Nonlinear dynamic	9 days 12 h
Non-restored case	Pushover G1-X	21 h
	Pushover G1-Y	20 h
	Nonlinear dynamic	11 days
Fully-restored case	Pushover G1-X	16 h
	Pushover G1-Y	15 h 30 min
	Nonlinear dynamic	7 days 12 h

nonlinearity was properly taken into account for both pushover and nonlinear dynamic analyses, in order have an insight into the possible reduction of strength due to resultant displacements outside the allowed range of applicability of linearity hypothesis.

Some words should be also spent for the isotropy hypothesis adopted for the masonry materials. While the adoption of isotropic strength domains for masonry is sometimes unrealistic (it is well known, indeed, that masonry behavior at failure is orthotropic [32]), in this particular case it may be fairly accepted, because masonry is constituted by multi-head (5–6 rows of standard Italian clay bricks) panels, with random but well distributed headers. The presence of such a pattern suggests that the utilization of both multi-leaf and complex orthotropic homogenization models could be equally questionable than the utilization of simple isotropic approaches, which are more robust and also in agreement with Italian code requirements.

It should be also pointed out that some other issues may be crucial, as for instance the role played by interlocking. This is an extremely complex question, which should be investigated with ad hoc numerical and local approaches, that by definition cannot be used in a global seismic characterization like the one presented in this paper.

As a matter of fact, standard modal, nonlinear static (pushover) and nonlinear dynamic analyses were performed on models with a huge number of Finite Elements. They are usually too demanding and sophisticated to be used in common design; however, the workstation used for these analyses presents 12 processors, and each analysis was performed by exploiting all of them, which allowed carrying out several computations, each requesting a relatively short amount of time, as shown in Table 7.

A final discussion merits the choice of material restoration instead of the utilization of classic rehabilitations done with tendons and tie rods. To increase globally masonry mechanical properties should be preferred in place of tendon utilization, as two main issues are to be considered in the latter case: the toothing quality of the tendons into the masonry (mainly due to the poor quality of the masonry itself) and the inherent local nature of such intervention, which may improve the seismic behavior locally while worsening it globally. Other interesting issues will be investigated in future companion papers, such as the presence of multi-leaf walls and transversal expected interlocking. Both matters are beyond the purpose of the present investigation and require, due to their complexity, ad hoc numerical approaches that cannot be used in a global seismic characterization like the one presented here.

6. Conclusions

A comprehensive numerical investigation has been carried out with the aim of better understanding the reasons behind the occurrence of diffused damages and local collapses on the historical masonry Castle of Finale Emilia, one of the symbols of the

devastation induced by the seismic sequence of 20–29th May 2012 in Emilia Romagna, Italy.

Two numerical models have been critically compared, with the additional aim of proposing an effective rehabilitation intervention that allows a sufficient protection against future damage induced by similar events. Two different meshes have been utilized and compared, one very refined and constituted by tetrahedron elements, the other much coarser and mainly constituted by hexahedrons. Three different hypotheses on the material have been done, the first corresponding to the real situation, where only the main façade exhibits improved mechanical properties, the second assuming the Castle as wholly non-restored, the last assuming the whole Castle restored.

From both pushover and nonlinear dynamic analyses, it has been found that, under the real situation, numerical damage patterns show several common features with the real ones. In particular, the West tower results totally collapsed in the upper part as a consequence of the activation of rocking partial failure mechanisms. Diffused damage is also found in the arches and vaults of the internal cloister, as well as non-negligible damage in the upper part of the remaining two towers. All such features are in good agreement with what observed in reality. Furthermore, the restored wall results almost undamaged, again in perfect agreement with the real behavior.

Interesting differences on the global behavior occur when assuming the original situation hypothesis. In such a case, indeed, the South-East wall (that was restored in 2009 but here is assumed with the same mechanical properties of the rest of the Castle) heavily damages mainly for in-plane shear actions. Towers and internal cloister result again generally collapsed, with a behavior quite similar to the one found in the real situation. It can be therefore stated that, despite very partial, the recent restoration intervention done was able to prevent further damage on the Castle, and hence it may be affirmed that it was rather beneficial, despite preserving only that part of the Castle subjected to mechanical upgrading.

To confirm such a conclusion, the numerical behavior of the Castle hypothetically fully restored shows reduced seismic vulnerability, with a state of damage limited to either the upper part of the towers or in presence of geometrical singularities (e.g. near the openings or at the intersection between perpendicular walls), that could also be justified by the approximations done during the discretization procedure or simply being a common consequence of local stress concentrations that cannot in any case influence the good global behavior of the structure under horizontal loads.

As far as seismic vulnerability is concerned, it has been shown that the restoration intervention executed in 2009 was able to increase the strength of the Castle along the direction parallel to the main façade (that works well under shear actions), thus preventing more diffused damages on it and in particular on its upper part. Conversely, an extension of the restoration interventions to the whole Castle would have greatly increased the strength of the structure on both directions, preventing to a great extent the damages on the upper parts of the three towers, as well as the local collapse on the West Tower. Under possible seismic sequences with a magnitude similar to that registered in 2012, the expected damages could be therefore mitigated, requiring minor restoration interventions limited to some details near the critical zones (singularities) linked to the complex geometry of the structure.

Acknowledgements

The authors would like to thank the anonymous reviewers for their valuable comments that have strongly improved the final quality of the paper.

References

[1] NTC 2008. Italian Ministry of Infrastructure and Transport. Italian Building Code-D.M. 14/01/2008. Rome, Italy, 2008 [in Italian].
[2] Circolare n° 617 del 2 febbraio 2009. Istruzioni per l'applicazione delle nuove norme tecniche per le costruzioni di cui al decreto ministeriale 14 gennaio; 2008 [Instructions for the application of the new technical norms on constructions].
[3] OPCM 3274/2003. Ordinanza del Presidente del Consiglio dei Ministri n. 3274 20/03/2003: Elementi in materia di criteri generali per la classificazione sismica del territorio nazionale e di normative tecniche per le costruzioni in zona sismica e successivi aggiornamenti.
[4] Linee guida per la valutazione e la riduzione del rischio sismico del patrimonio culturale. Italy: Ministero per i beni e le attività culturali MiBAC; 2011.
[5] Milani G. Lesson learned after the Emilia Romagna, Italy, 20–29 May 2012 earthquakes: a limit analysis insight on three masonry churches. Eng Fail Anal 2013;34:761–78.
[6] Betti M, Vignoli A. Numerical assessment of the static and seismic behaviour of the basilica of Santa Maria all'Impruneta (Italy). Constr Build Mater 2011;25:4308–24.
[7] Brandonisio G, Lucibello G, Mele E, De Luca A. Damage and performance evaluation of masonry churches in the 2009 L'Aquila earthquake. Eng Fail Anal 2011;34:693–714.
[8] Milani G, Venturini G. Automatic fragility curve evaluation of masonry churches accounting for partial collapses by means of 3D FE homogenized limit analysis. Comput Struct 2011;89:1628–48.
[9] Augusti G, Ciampoli M, Zanobi S. Bounds to the probability of collapse of monumental buildings. Struct Saf 2002;24:89–105.
[10] Lourenço PB, Roque JA. Simplified indexes for the seismic vulnerability of ancient masonry buildings. Constr Build Mater 2006;20:200–8.
[11] Foraboschi P. Church of San Giuliano di Puglia: seismic repair and upgrading. Eng Fail Anal 2013;33:281–314.
[12] Cattari S, Abbati SD, Ferretti D, Lagomarsino S, Ottonelli D, Tralli A. Damage assessment of fortresses after the 2012 Emilia earthquake (Italy). Bull Earthq Eng 2014;12(5):2333–65.
[13] Binda L, Modena C, Casarin F, Lorenzoni F, Cantini L, Munda S. Emergency actions and investigations on cultural heritage after the L'Aquila earthquake: the case of the Spanish Fortress. Bull Earthq Eng 2011;9(1):105–38.
[14] Lucibello G, Brandonisio G, Mele E, De Luca A. Seismic damage and performance of Palazzo Centi after L'Aquila earthquake: a paradigmatic case study of effectiveness of mechanical steel ties. Eng Fail Anal 2011;34: 407–30.
[15] Betti M, Orlando M, Vignoli A. Static behaviour of an Italian Medieval Castle: damage assessment by numerical modelling. Comput Struct 2011;89: 1956–70.
[16] Lagomarsino S, Resemini S. The assessment of damage limitation state in the seismic analysis of monumental buildings. Earthq Spectra 2009;25(2):323–46.
[17] Ramos L, Lourenço PB. Modeling and vulnerability of historical city centers in seismic areas: a case study in Lisbon. Eng Struct 2004;26:1295–310.
[18] Barbieri G, Biolzi L, Bocciarelli M, Fregonese L, Frigeri A. Assessing the seismic vulnerability of a historical building. Eng Struct 2013;57:523–35.
[19] Acito M, Bocciarelli M, Chesi C, Milani G. Collapse of the clock tower in Finale Emilia after the May 2012 Emilia Romagna earthquake sequence: numerical insight. Eng Struct 2014;72:70–91.
[20] Ramos L, Lourenço PB. Modeling and vulnerability of historical city centers in seismic areas: a case study in Lisbon. Eng Struct 2004;26(9):1295–310.
[21] Bento R, Lopes M, Cardoso R. Seismic evaluation of old masonry buildings. Part II: analysis of strengthening solutions for a case study. Eng Struct 2005;27 (14):2014–23.
[22] Lourenço PB, Mendes N, Ramos LF, Oliveira DV. Analysis of masonry structures without box behaviour. Int J Architectural Herit 2011;4–5:369–82.
[23] Endo Y, Pelà L, Roca P, da Porto F, Modena C. Comparison of seismic analysis methods applied to a historical church struck by 2009 L'Aquila earthquake. Bull Earthq Eng 2015;13(12):3749–78.
[24] Bellei S, Rovatti E. Castelli Modenesi della Pianura. Finale Emilia (Italy): Collezioni Modenesi; 2000 [in Italian].
[25] Calzolari M, Righini M, Tusini GL. Le rocche di Finale in età Estense. Secoli XIV–XVI. San Felice sul Panaro (Modena, Italy): Editore Gruppo Studi Bassa Modenese; 2009 [in Italian].
[26] Strand7®. Theoretical manual-theoretical background to the Strand7 finite element analysis system; 2008.
[27] ABAQUS®. Theory manual. Version 6.13-2; 2013.
[28] Alessandri C, Di Francesco C, Guerzoni G. L'abbazia di Pomposa: analisi di un dissesto statico e proposta di consolidamento. Costruire in Laterizio 2000;74:48–53.
[29] Borri A, Cangi G, De Maria A. Caratterizzazione meccanica delle murature (anche alla luce del recente sisma in Emilia) e interpretazione delle prove sperimentali a taglio. In Proc: ANIDIS Congress Associazione Nazionale Italiana Di Ingegneria Sismica, Padua, 30 June–4 July 2013; 2013.
[30] Binda L, Tiraboschi C, Mirabella Roberti G, Baronio G, Cardani G. Experimental and numerical investigation on a brick masonry building prototype: Part 1. Technical University of Milan, internal report, Milan, Italy; 1995.
[31] Binda L, Tiraboschi C, Mirabella Roberti G, Baronio G, Cardani G. Experimental and numerical investigation on a brick masonry building prototype: Part 2. Technical University of Milan, internal report, Milan, Italy; 1995.

[32] Milani G, Lourenco PB, Tralli A. Homogenised limit analysis of masonry walls, Part I: failure surfaces. Comput Struct 2006;84(3–4):166–80.
[33] Lubliner J, Oliver J, Oller S, Oñate E. A plastic-damage model for concrete. Int J Solids Struct 1989;25(3):299–326.
[34] Van Zijl G. Modeling masonry shear-compression: role of dilatancy highlighted. J Eng Mech, ASCE 2004;130(11):1289–96.
[35] Minghini F, Milani G, Tralli A. Seismic risk assessment of a 50 m high masonry chimney using advanced analysis techniques. Eng Struct 2014;69:255–70.
[36] Choudhury T, Milani G, Kaushik HB. Comprehensive numerical approaches for the design and safety assessment of retrofitted masonry buildings with steel bands in developing countries: the case of India. Constr Build Mater 2015;85:227–46. http://dx.doi.org/10.1016/j.conbuildmat.2015.02.082.
[37] Allemang RJ. The modal assurance criterion – twenty years of use and abuse. Sound Vib 2003 [August: 14–21].
[38] Milani G, Valente M. Comparative pushover and limit analyses on seven masonry churches damaged by the 2012 Emilia-Romagna (Italy) seismic events: possibilities of non-linear Finite Elements compared with pre-assigned failure mechanisms. Eng. Fail. Anal. 2015;47:129–61.
[39] Pelà L, Aprile A, Benedetti A. Seismic assessment of masonry arch bridges. Eng Struct 2009;31(8):1777–88.
[40] Fajfar P. A nonlinear analysis method for performance-based seismic design. Earthq Spectra 2000;16(3):573–92.